

Search for new phenomena with the M_{T2} variable in the all-hadronic final state produced in proton–proton collisions at $\sqrt{s} = 13$ TeV

CMS Collaboration*

CERN, 1211 Geneva 23, Switzerland

Received: 12 May 2017 / Accepted: 26 September 2017 / Published online: 26 October 2017
© CERN for the benefit of the CMS collaboration 2017. This article is an open access publication

Abstract A search for new phenomena is performed using events with jets and significant transverse momentum imbalance, as inferred through the M_{T2} variable. The results are based on a sample of proton–proton collisions collected in 2016 at a center-of-mass energy of 13 TeV with the CMS detector and corresponding to an integrated luminosity of 35.9 fb^{-1} . No excess event yield is observed above the predicted standard model background, and the results are interpreted as exclusion limits at 95% confidence level on the masses of predicted particles in a variety of simplified models of R -parity conserving supersymmetry. Depending on the details of the model, 95% confidence level lower limits on the gluino (light-flavor squark) masses are placed up to 2025 (1550) GeV. Mass limits as high as 1070 (1175) GeV are set on the masses of top (bottom) squarks. Information is provided to enable re-interpretation of these results, including model-independent limits on the number of non-standard model events for a set of simplified, inclusive search regions.

1 Introduction

We present results of a search for new phenomena in events with jets and significant transverse momentum imbalance in proton–proton collisions at $\sqrt{s} = 13$ TeV. Such searches were previously conducted by both the ATLAS [1–5] and CMS [6–9] Collaborations. Our search builds on the work presented in Ref. [6], using improved methods to estimate the background from standard model (SM) processes and a data set corresponding to an integrated luminosity of 35.9 fb^{-1} of pp collisions collected during 2016 with the CMS detector at the CERN LHC. Event counts in bins of the number of jets (N_j), the number of b-tagged jets (N_b), the scalar sum of the transverse momenta p_T of all selected jets (H_T), and the M_{T2} variable [6, 10] are compared against estimates of the background from SM processes derived from dedicated data

control samples. We observe no evidence for a significant excess above the expected background event yield and interpret the results as exclusion limits at 95% confidence level on the production of pairs of gluinos and squarks using simplified models of supersymmetry (SUSY) [11–18]. Model-independent limits on the number of non-SM events are also provided for a simpler set of inclusive search regions.

2 The CMS detector

The central feature of the CMS apparatus is a superconducting solenoid of 6 m internal diameter, providing a magnetic field of 3.8 T. Within the solenoid volume are a silicon pixel and strip tracker, a lead tungstate crystal electromagnetic calorimeter, and a brass and scintillator hadron calorimeter, each composed of a barrel and two endcap sections. Forward calorimeters extend the pseudorapidity (η) coverage provided by the barrel and endcap detectors. Muons are measured in gas-ionization detectors embedded in the steel flux-return yoke outside the solenoid. The first level of the CMS trigger system, composed of custom hardware processors, uses information from the calorimeters and muon detectors to select the most interesting events in a fixed time interval of less than $4 \mu\text{s}$. The high-level trigger processor farm further decreases the event rate from around 100 kHz to less than 1 kHz, before data storage. A more detailed description of the CMS detector and trigger system, together with a definition of the coordinate system used and the relevant kinematic variables, can be found in Refs. [19, 20].

3 Event selection and Monte Carlo simulation

Events are processed using the particle-flow (PF) algorithm [21], which is designed to reconstruct and identify all particles using the optimal combination of information

* e-mail: cms-publication-committee-chair@cern.ch

Table 1 Summary of reconstruction objects and event preselection. Here R is the distance parameter of the anti- k_T algorithm. For veto leptons and tracks, the transverse mass M_T is determined using the veto object and the \vec{p}_T^{miss} . The variable p_T^{sum} is a measure of isolation and it denotes the sum of the transverse momenta of all the PF candidates in a cone around the lepton or the track. The size of the cone, in units of $\Delta R \equiv \sqrt{(\Delta\phi)^2 + (\Delta\eta)^2}$ is given in the table. Further details of the lepton selection are described in Ref. [6]. The i th highest- p_T jet is denoted as j_i

Trigger	$p_T^{\text{miss}} > 120 \text{ GeV}$ and $H_T^{\text{miss}} > 120 \text{ GeV}$ or $H_T > 300 \text{ GeV}$ and $p_T^{\text{miss}} > 110 \text{ GeV}$ or $H_T > 900 \text{ GeV}$ or jet $p_T > 450 \text{ GeV}$
Jet selection	$R = 0.4$, $p_T > 30 \text{ GeV}$, $ \eta < 2.4$
b tag selection	$p_T > 20 \text{ GeV}$, $ \eta < 2.4$
p_T^{miss}	$p_T^{\text{miss}} > 250 \text{ GeV}$ for $H_T < 1000 \text{ GeV}$, else $p_T^{\text{miss}} > 30 \text{ GeV}$ $\Delta\phi_{\text{min}} = \Delta\phi(p_T^{\text{miss}}, j_{1,2,3,4}) > 0.3$ $ \vec{p}_T^{\text{miss}} - \vec{H}_T^{\text{miss}} /p_T^{\text{miss}} < 0.5$
M_{T2}	$M_{T2} > 200 \text{ GeV}$ for $H_T < 1500 \text{ GeV}$, else $M_{T2} > 400 \text{ GeV}$
Veto muon	$p_T > 10 \text{ GeV}$, $ \eta < 2.4$, $p_T^{\text{sum}} < 0.2 p_T^{\text{lep}}$ or $p_T > 5 \text{ GeV}$, $ \eta < 2.4$, $M_T < 100 \text{ GeV}$, $p_T^{\text{sum}} < 0.2 p_T^{\text{lep}}$
Veto electron	$p_T > 10 \text{ GeV}$, $ \eta < 2.4$, $p_T^{\text{sum}} < 0.1 p_T^{\text{lep}}$ or $p_T > 5 \text{ GeV}$, $ \eta < 2.4$, $M_T < 100 \text{ GeV}$, $p_T^{\text{sum}} < 0.2 p_T^{\text{lep}}$
Veto track	$p_T > 10 \text{ GeV}$, $ \eta < 2.4$, $M_T < 100 \text{ GeV}$, $p_T^{\text{sum}} < 0.1 p_T^{\text{track}}$
p_T^{sum} cone	Veto e or μ : $\Delta R = \min(0.2, \max(10 \text{ GeV}/p_T^{\text{lep}}, 0.05))$ Veto track: $\Delta R = 0.3$

from the elements of the CMS detector. Physics objects reconstructed with this algorithm are hereafter referred to as particle-flow candidates. The physics objects and the event preselection are similar to those described in Ref. [6], and are summarized in Table 1. We select events with at least one jet, and veto events with an isolated lepton (e or μ) or charged PF candidate. The isolated charged PF candidate selection is designed to provide additional rejection against events with electrons and muons, as well as to reject hadronic tau decays. Jets are formed by clustering PF candidates using the anti- k_T algorithm [22, 23] and are corrected for contributions from event pileup [24] and the effects of non-uniform detector response. Only jets passing the selection criteria in Table 1 are used for counting and the determination of kinematic variables. Jets consistent with originating from a heavy-flavor hadron are identified using the combined secondary vertex tagging algorithm [25], with a working point chosen such that the efficiency to identify a b quark jet is in the range 50–65% for jet p_T between 20 and 400 GeV. The misidentification rate is approximately 1% for light-flavor and gluon jets and 10% for charm jets. A more detailed discussion of the algorithm performance is given in Ref. [25].

The negative of the vector sum of the p_T of all selected jets is denoted by \vec{H}_T^{miss} , while \vec{p}_T^{miss} is defined as the negative of the vector p_T sum of all reconstructed PF candidates. The jet corrections are also used to correct \vec{p}_T^{miss} . Events with possible contributions from beam-halo processes or anomalous noise in the calorimeter are rejected using dedicated filters [26, 27]. For events with at least two jets, we start with the pair having the largest dijet invariant mass and iteratively cluster all selected jets using a hemisphere algorithm that minimizes the Lund distance measure [28, 29] until two stable

pseudo-jets are obtained. The resulting pseudo-jets together with the \vec{p}_T^{miss} are used to calculate the kinematic variable M_{T2} as:

$$M_{T2} = \min_{\vec{p}_T^{\text{miss}X(1)} + \vec{p}_T^{\text{miss}X(2)} = \vec{p}_T^{\text{miss}}} \left[\max \left(M_T^{(1)}, M_T^{(2)} \right) \right], \quad (1)$$

where $\vec{p}_T^{\text{miss}X(i)}$ ($i = 1, 2$) are trial vectors obtained by decomposing \vec{p}_T^{miss} , and $M_T^{(i)}$ are the transverse masses obtained by pairing either of the trial vectors with one of the two pseudo-jets. The minimization is performed over all trial momenta satisfying the \vec{p}_T^{miss} constraint. The background from multijet events (discussed in Sect. 4) is characterized by small values of M_{T2} , while larger M_{T2} values are obtained in processes with significant, genuine \vec{p}_T^{miss} .

Collision events are selected using triggers with requirements on H_T , p_T^{miss} , H_T^{miss} , and jet p_T . The combined trigger efficiency, as measured in a data sample of events with an isolated electron, is found to be $> 98\%$ across the full kinematic range of the search. To suppress background from multijet production, we require $M_{T2} > 200 \text{ GeV}$ in events with $N_j \geq 2$ and $H_T < 1500 \text{ GeV}$. This M_{T2} threshold is increased to 400 GeV for events with $H_T > 1500 \text{ GeV}$ to maintain multijet processes as a subdominant background in all search regions. To protect against jet mismeasurement, we require the minimum difference in azimuthal angle between the \vec{p}_T^{miss} vector and each of the leading four jets, $\Delta\phi_{\text{min}}$, to be greater than 0.3, and the magnitude of the difference between \vec{p}_T^{miss} and \vec{H}_T^{miss} to be less than half of p_T^{miss} . For the determination of $\Delta\phi_{\text{min}}$ we consider jets with $|\eta| < 4.7$. If less than four such jets are found, all are considered in the $\Delta\phi_{\text{min}}$ calculation.

Events containing at least two jets are categorized by the values of N_j , N_b , and H_T . Each such bin is referred to as a *topological region*. Signal regions are defined by further dividing topological regions into bins of M_{T2} . Events with only one jet are selected if the p_T of the jet is at least 250 GeV, and are classified according to the p_T of this jet and whether the event contains a b-tagged jet. The search regions are summarized in Tables 5, 6, 7 in Appendix A. We also define *super signal regions*, covering a subset of the kinematic space of the full analysis with simpler inclusive selections. The super signal regions can be used to obtain approximate interpretations of our result, as discussed in Sect. 5, where these regions are defined.

Monte Carlo (MC) simulations are used to design the search, to aid in the estimation of SM backgrounds, and to evaluate the sensitivity to gluino and squark pair production in simplified models of SUSY. The main background samples (Z+jets, W+jets, and $t\bar{t}$ +jets), as well as signal samples of gluino and squark pair production, are generated at leading order (LO) precision with the MADGRAPH 5 generator [30,31] interfaced with PYTHIA 8.2 [32] for fragmentation and parton showering. Up to four, three, or two additional partons are considered in the matrix element calculations for the generation of the V+jets ($V = Z, W$), $t\bar{t}$ +jets, and signal samples, respectively. Other background processes are also considered: $t\bar{t}V$ ($V = Z, W$) samples are generated at LO precision with the MADGRAPH 5 generator, with up to two additional partons in the matrix element calculations, while single top samples are generated at next-to-leading order (NLO) precision with the MADGRAPH_aMC@NLO [30] or POWHEG [33,34] generators. Contributions from rarer processes such as diboson, triboson, and four top production, are found to be negligible. Standard model samples are simulated with a detailed GEANT4 [35] based detector simulation and processed using the same chain of reconstruction programs as collision data, while the CMS fast simulation program [36] is used for the signal samples. The most precise available cross section calculations are used to normalize the simulated samples, corresponding most often to NLO or next-to-NLO accuracy [30,33,34,37–40].

To improve on the MADGRAPH modeling of the multiplicity of additional jets from initial state radiation (ISR), MADGRAPH $t\bar{t}$ MC events are weighted based on the number of ISR jets (N_j^{ISR}) so as to make the jet multiplicity agree with data. The same reweighting procedure is applied to SUSY MC events. The weighting factors are obtained from a control region enriched in $t\bar{t}$, obtained by selecting events with two leptons and exactly two b-tagged jets, and vary between 0.92 for $N_j^{ISR} = 1$ and 0.51 for $N_j^{ISR} \geq 6$. We take one half of the deviation from unity as the systematic uncertainty in these reweighting factors, to cover for differences between $t\bar{t}$ and SUSY production.

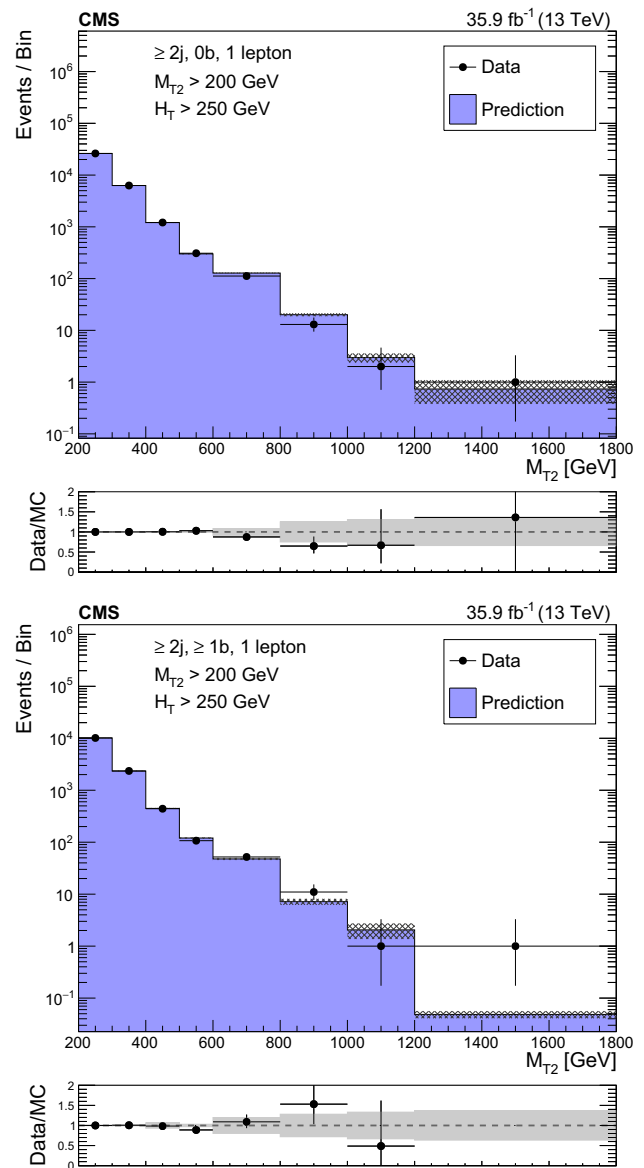


Fig. 1 Distributions of the M_{T2} variable in data and simulation for the single-lepton control region selection, after normalizing the simulation to data in the control region bins of H_T , N_j , and N_b for events with no b-tagged jets (upper), and events with at least one b-tagged jet (lower). The hatched bands on the top panels show the MC statistical uncertainty, while the solid gray bands in the ratio plots show the systematic uncertainty in the M_{T2} shape

4 Backgrounds

The backgrounds in jets-plus- p_T^{miss} final states typically arise from three categories of SM processes:

- “lost lepton (LL)”, i.e., events with a lepton from a W decay where the lepton is either out of acceptance, not reconstructed, not identified, or not isolated. This background originates mostly from W+jets and

$t\bar{t}$ +jets events, with smaller contributions from rarer processes such as diboson or $t\bar{t}V$ ($V = Z, W$) production.

- “irreducible”, i.e., Z +jets events, where the Z boson decays to neutrinos. This background is most similar to potential signals. It is a major background in nearly all search regions, its importance decreasing with increasing N_b .
- “instrumental background”, i.e., mostly multijet events with no genuine p_T^{miss} . These events enter a search region due to either significant jet momentum mismeasurements, or sources of anomalous noise.

4.1 Estimation of the background from events with leptonic W boson decays

Control regions with exactly one lepton candidate are selected using the same triggers and preselections used for the signal regions, with the exception of the lepton veto, which is inverted. Selected events are binned according to the same criteria as the search regions, and the background in each signal bin, N_{LL}^{SR} , is obtained from the number of events in the control region, $N_{1\ell}^{\text{CR}}$, using transfer factors according to:

$$\begin{aligned}
 N_{LL}^{\text{SR}}(H_T, N_j, N_b, M_{T2}) &= N_{1\ell}^{\text{CR}}(H_T, N_j, N_b, M_{T2}) \\
 &\times R_{\text{MC}}^{0\ell/1\ell}(H_T, N_j, N_b, M_{T2}) k(M_{T2}). \tag{2}
 \end{aligned}$$

The single-lepton control region typically has 1–2 times as many events as the corresponding signal region. The factor $R_{\text{MC}}^{0\ell/1\ell}(H_T, N_j, N_b, M_{T2})$ accounts for lepton acceptance and efficiency and the expected contribution from the decay of W bosons to hadrons through an intermediate τ lepton. It is obtained from MC simulation, and corrected for measured differences in lepton efficiencies between data and simulation.

The factor $k(M_{T2})$ accounts for the distribution, in bins of M_{T2} , of the estimated background in each topological region. It is obtained using both data and simulation as follows. In each topological region, the control region corresponding to the highest M_{T2} bin is successively combined with the next highest bin until the expected SM yield in combined bins is at least 50 events. When two or more control region bins are combined, the fraction of events expected to populate a particular M_{T2} bin, $k(M_{T2})$, is determined using the expectation from SM simulated samples, including all relevant processes. The modeling of M_{T2} is checked in data using single-lepton control samples enriched in events originating from either W +jets or $t\bar{t}$ +jets, as shown in the upper and lower panels of Fig. 1, respectively. The predicted distributions in the comparison are obtained by summing all control regions after normalizing MC yields to data and distributing events among M_{T2} bins according to the expectation from simulation, as is done for the estimate of the lost-lepton background. For

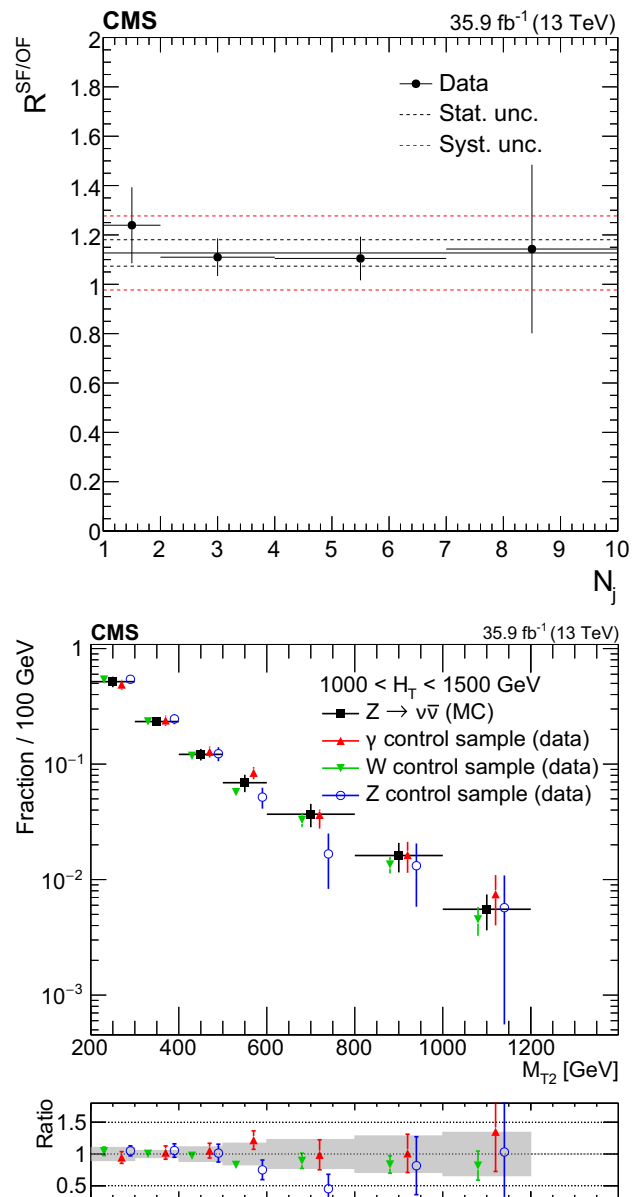


Fig. 2 (Upper) Ratio $R^{\text{SF/OF}}$ in data as a function of N_j . The solid black line enclosed by the red dashed lines corresponds to a value of 1.13 ± 0.15 that is observed to be stable with respect to event kinematics, while the two dashed black lines denote the statistical uncertainty in the $R^{\text{SF/OF}}$ value. (Lower) The shape of the M_{T2} distribution in $Z \rightarrow \nu\bar{\nu}$ simulation compared to shapes from γ , W , and Z data control samples in a region with $1000 < H_T < 1500$ GeV and $N_j \geq 2$, inclusive in N_b . The solid gray band on the ratio plot shows the systematic uncertainty in the M_{T2} shape

events with $N_j = 1$, a control region is defined for each bin of jet p_T .

Uncertainties from the limited size of the control sample and from theoretical and experimental sources are evaluated and propagated to the final estimate. The dominant uncertainty in $R_{\text{MC}}^{0\ell/1\ell}(H_T, N_j, N_b, M_{T2})$ arises from the modeling of the lepton efficiency (for electrons, muons, and

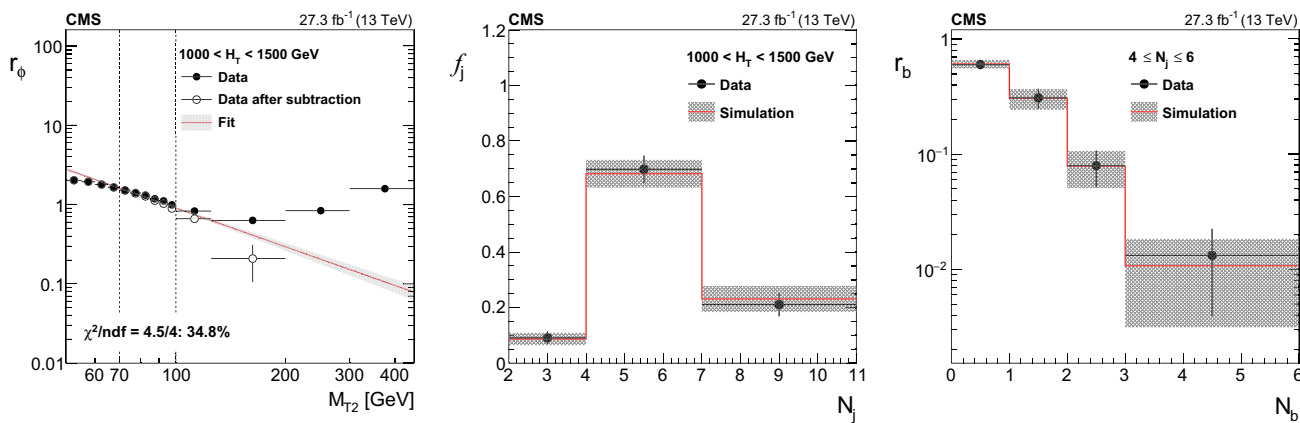


Fig. 3 The ratio r_ϕ as a function of M_{T2} for $1000 < H_T < 1500$ GeV (left). The superimposed fit is performed to the open circle data points. The black points represent the data before subtracting non-multijet contributions using simulation. Data point uncertainties are statistical only. The red line and the grey band around it show the result of the fit to a power-law function performed in the window $70 < M_{T2} < 100$ GeV

hadronically-decaying tau leptons) and jet energy scale (JES) and is of order 15–20%. The uncertainty in the M_{T2} extrapolation, which is as large as 40%, arises primarily from the JES, the relative fractions of W+jets and $t\bar{t}$ +jets, and variations of the renormalization and factorization scales assumed for their simulation. These and other uncertainties are similar to those in Ref. [6].

4.2 Estimation of the background from $Z(\nu\bar{\nu})$ +jets

The $Z \rightarrow \nu\bar{\nu}$ background is estimated from a dilepton control sample selected using triggers requiring two leptons. The trigger efficiency, measured with a data sample of events with large H_T , is found to be greater than 97% in the selected kinematic range. To obtain a control sample enriched in $Z \rightarrow \ell^+\ell^-$ events ($\ell = e, \mu$), we require that the leptons are of the same flavor, opposite charge, that the p_T of the leading and trailing leptons are at least 100 and 30 GeV, respectively, and that the invariant mass of the lepton pair is consistent with the mass of a Z boson within 20 GeV. After requiring that the p_T of the dilepton system is at least 200 GeV, the preselection requirements are applied based on kinematic variables recalculated after removing the dilepton system from the event to replicate the $Z \rightarrow \nu\bar{\nu}$ kinematics. For events with $N_j = 1$, one control region is defined for each bin of jet p_T . For events with at least two jets, the selected events are binned in H_T , N_j , and N_b , but not in M_{T2} , to increase the dilepton event yield in each control region.

The contribution to each control region from flavor-symmetric processes, most importantly $t\bar{t}$, is estimated using opposite-flavor (OF) $e\mu$ events obtained with the same selections as same-flavor (SF) ee and $\mu\mu$ events. The background in each signal bin is then obtained using transfer factors

and the associated fit uncertainty. Values of f_j , the fraction of events in bin N_j , (middle) and r_b , the fraction of events in bin N_b that fall in data after requiring $\Delta\phi_{\min} < 0.3$ and $100 < M_{T2} < 200$ GeV. The hatched bands represent both statistical and systematic uncertainties

according to:

$$\begin{aligned}
 N_{Z \rightarrow \nu\bar{\nu}}^{\text{SR}}(H_T, N_j, N_b, M_{T2}) &= \left[N_{\ell\ell}^{\text{CRSF}}(H_T, N_j, N_b) - N_{\ell\ell}^{\text{CROF}}(H_T, N_j, N_b) R^{\text{SF/OF}} \right] \\
 &\times R_{\text{MC}}^{Z \rightarrow \nu\bar{\nu}/Z \rightarrow \ell^+\ell^-}(H_T, N_j, N_b) k(M_{T2}). \tag{3}
 \end{aligned}$$

Here $N_{\ell\ell}^{\text{CRSF}}$ and $N_{\ell\ell}^{\text{CROF}}$ are the number of SF and OF events in the control region, while $R_{\text{MC}}^{Z \rightarrow \nu\bar{\nu}/Z \rightarrow \ell^+\ell^-}$ and $k(M_{T2})$ are defined below. The factor $R^{\text{SF/OF}}$ accounts for the difference in acceptance and efficiency between SF and OF events. It is determined as the ratio of the number of SF events to OF events in a $t\bar{t}$ enriched control sample, obtained with the same selections as the $Z \rightarrow \ell^+\ell^-$ sample, but inverting the requirements on the p_T and the invariant mass of the lepton pair. A measured value of $R^{\text{SF/OF}} = 1.13 \pm 0.15$ is observed to be stable with respect to event kinematics, and is applied in all regions. Figure 2 (left) shows $R^{\text{SF/OF}}$ measured as a function of the number of jets.

An estimate of the $Z \rightarrow \nu\bar{\nu}$ background in each topological region is obtained from the corresponding dilepton control region via the factor $R_{\text{MC}}^{Z \rightarrow \nu\bar{\nu}/Z \rightarrow \ell^+\ell^-}$, which accounts for the acceptance and efficiency to select the dilepton pair and the ratio of branching fractions for $Z \rightarrow \ell^+\ell^-$ and $Z \rightarrow \nu\bar{\nu}$ decays. This factor is obtained from simulation, including corrections for differences in the lepton efficiencies between data and simulation.

The factor $k(M_{T2})$ accounts for the distribution, in bins of M_{T2} , of the estimated background in each topological region. This distribution is constructed using the M_{T2} shape from dilepton data and $Z \rightarrow \nu\bar{\nu}$ simulation in each topological region. Studies with simulated samples indicate that the M_{T2} shape for $Z \rightarrow \nu\bar{\nu}$ events is inde-

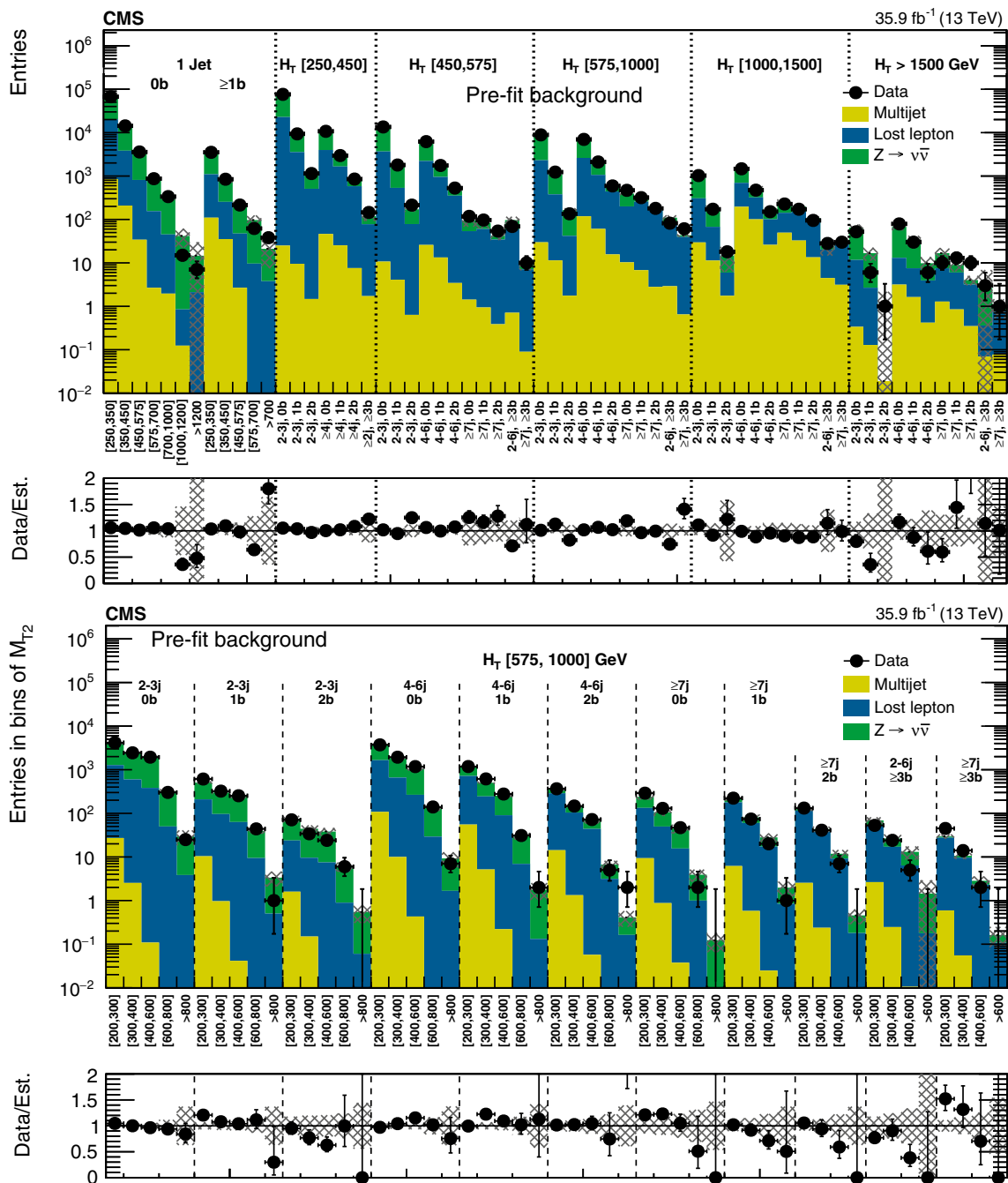


Fig. 4 (Upper) Comparison of estimated (pre-fit) background and observed data events in each topological region. Hatched bands represent the full uncertainty in the background estimate. The results shown for $N_j = 1$ correspond to the monojet search regions binned in jet p_T ,

whereas for the multijet signal regions, the notations j, b indicate N_j, N_b labeling. (Lower) Same for individual M_{T2} signal bins in the medium H_T region. On the x -axis, the M_{T2} binning is shown in units of GeV

pendent of N_b for a given H_T and N_j selection, and that the shape is also independent of the number of jets for $H_T > 1500$ GeV. The MC modeling of N_b and N_j as well as of the M_{T2} shape in bins of N_j and N_b is validated in data, using a dilepton control sample. As a result, M_{T2} templates for topological regions differing only in N_b are

combined, separately for data and simulation. For $H_T > 1500$ GeV, only one M_{T2} template is constructed for data and one for simulation by combining all relevant topological regions.

Starting from the highest M_{T2} bin in each control region, we merge bins until the sum of the merged bins contains

Table 2 Definitions of super signal regions, along with predictions, observed data, and the observed 95% CL upper limits on the number of signal events contributing to each region (N_{95}^{obs}). The limits are shown as a range corresponding to an assumed uncertainty in the signal acceptance of 0–15%. A dash in the selections means that no requirement is applied

Region	N_j	N_b	H_T (GeV)	M_{T2} (GeV)	Prediction	Data	N_{95}^{obs}
2j loose	≥ 2	—	> 1000	> 1200	38.9 ± 11.2	42	26.6–27.8
2j tight	≥ 2	—	> 1500	> 1400	2.9 ± 1.3	4	6.5–6.7
4j loose	≥ 4	—	> 1000	> 1000	19.4 ± 5.8	21	15.8–16.4
4j tight	≥ 4	—	> 1500	> 1400	2.1 ± 0.9	2	4.4–4.6
7j loose	≥ 7	—	> 1000	> 600	$23.5^{+5.9}_{-5.6}$	27	18.0–18.7
7j tight	≥ 7	—	> 1500	> 800	$3.1^{+1.7}_{-1.4}$	5	7.6–7.9
2b loose	≥ 2	≥ 2	> 1000	> 600	$12.9^{+2.9}_{-2.6}$	16	12.5–13.0
2b tight	≥ 2	≥ 2	> 1500	> 600	$5.1^{+2.7}_{-2.1}$	4	5.8–6.0
3b loose	≥ 2	≥ 3	> 1000	> 400	8.4 ± 1.8	10	9.3–9.7
3b tight	≥ 2	≥ 3	> 1500	> 400	2.0 ± 0.6	4	6.6–6.9
7j3b loose	≥ 7	≥ 3	> 1000	> 400	5.1 ± 1.5	5	6.4–6.6
7j3b tight	≥ 7	≥ 3	> 1500	> 400	0.9 ± 0.5	1	3.6–3.7

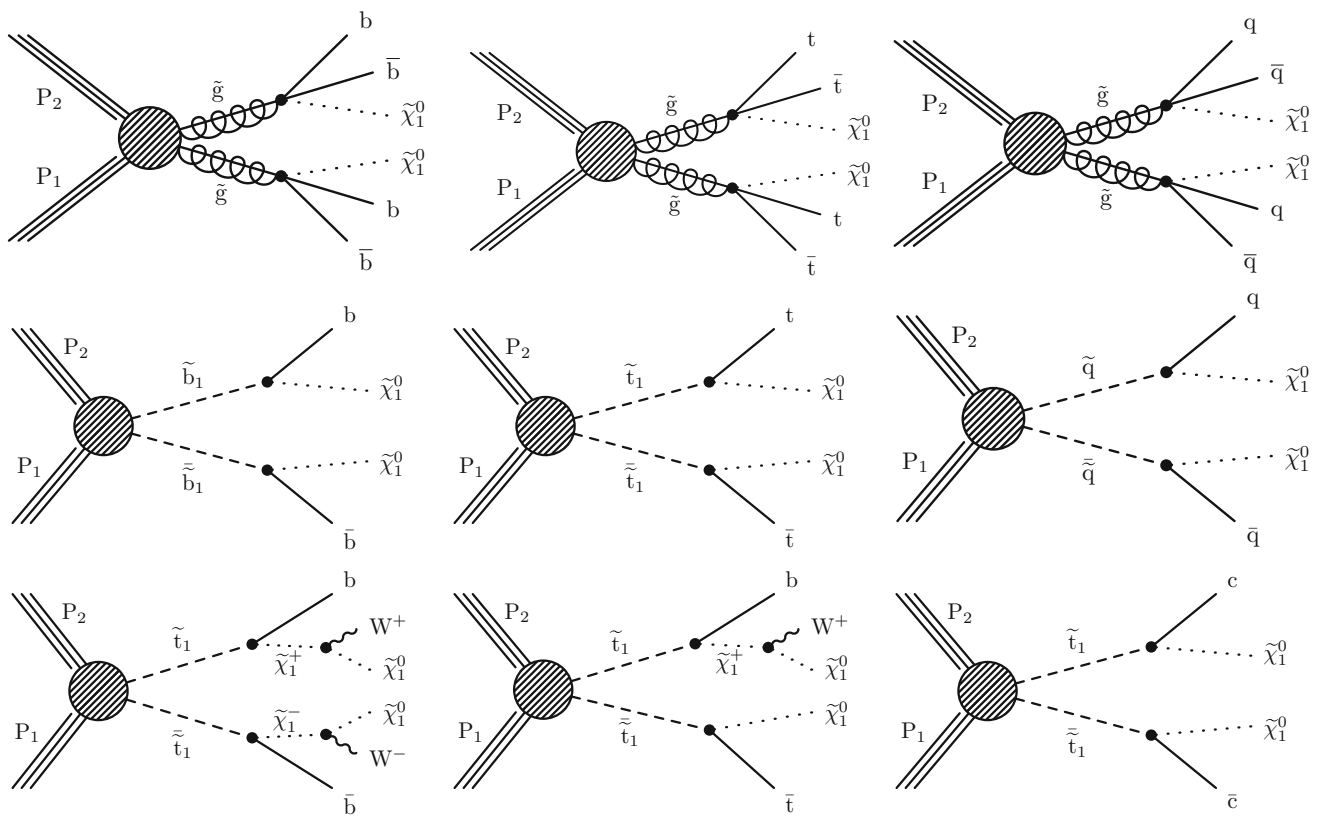


Fig. 5 (Upper) Diagrams for the three scenarios of gluino-mediated bottom squark, top squark and light flavor squark production considered. (Middle) Diagrams for the direct production of bottom, top and light-flavor squark pairs. (Lower) Diagrams for three alternate scenarios

of direct top squark production with different decay modes. For mixed decay scenarios, we assume a 50% branching fraction for each decay mode

at least 50 expected events from simulation. The fraction of events in each uncombined bin is determined using the corresponding M_{T2} template from dilepton data, corrected by the ratio $R_{MC}^{Z \rightarrow \nu\bar{\nu}/Z \rightarrow \ell^+\ell^-}$. The M_{T2} shape from simulation is used to distribute events among the combined bins, after nor-

malizing the simulation to the data yield in the same group of bins.

The modeling of M_{T2} is validated in data using control samples enriched in γ , $W \rightarrow \ell\nu$, and $Z \rightarrow \ell^+\ell^-$ events in each bin of H_T . The lower panel of Fig. 2 shows agree-

Table 3 Typical values of the systematic uncertainties as evaluated for the simplified models of SUSY used in the context of this search. The high statistical uncertainty in the simulated signal sample corresponds to a small number of signal bins with low acceptance, which are typically not among the most sensitive signal bins to that model point.

Source	Typical values (%)
Integrated luminosity	2.5
Limited size of MC samples	1–100
Renormalization and factorization scales	5
ISR modeling	0–30
b Tagging efficiency, heavy flavors	0–40
b Tagging efficiency, light flavors	0–20
Lepton efficiency	0–20
Jet energy scale	5
Fast simulation p_T^{miss} modeling	0–5
Fast simulation pileup modeling	4.6

ment between the M_{T2} distributions obtained from γ , W, and Z data control samples with that from $Z \rightarrow \nu\bar{\nu}$ simulation for events with $1000 < H_T < 1500$ GeV. In this comparison, the γ sample is obtained by selecting events with $p_T^\gamma > 180$ GeV and is corrected for contributions from multijet events and $R_{MC}^{Z/\gamma}$, the W sample is corrected for $R_{MC}^{Z/W}$, both the W and Z samples are corrected for contributions from top quark events, and the Z sample is further corrected for $R_{MC}^{Z \rightarrow \nu\bar{\nu}/Z \rightarrow \ell^+\ell^-}$. Here $R_{MC}^{Z/\gamma}$ ($R_{MC}^{Z/W}$) is the ratio of the M_{T2} distributions for Z boson and γ (W) boson events derived in simulation.

The largest uncertainty in the estimate of the invisible Z background in most regions results from the limited size of the dilepton control sample. This uncertainty, as well as all other relevant theoretical and experimental uncertainties, are evaluated and propagated to the final estimate. The dominant uncertainty in the ratio $R_{MC}^{Z \rightarrow \nu\bar{\nu}/Z \rightarrow \ell^+\ell^-}$ is obtained from measured differences in lepton efficiency between data and simulation, and is about 5%. The uncertainty in the k (M_{T2}) factor arises from data statistics for uncombined bins, while for combined bins it is due to uncertainties in the JES and variations in the renormalization and factorization scales. These can result in effects as large as 40%.

4.3 Estimation of the multijet background

For events with at least two jets, a multijet-enriched control region is obtained in each H_T bin by inverting the $\Delta\phi_{\min}$ requirement described in Sect. 3. Events are selected using H_T triggers, and the extrapolation from low- to high- $\Delta\phi_{\min}$ is based on the following ratio:

$$r_\phi(M_{T2}) = N(\Delta\phi_{\min} > 0.3)/N(\Delta\phi_{\min} < 0.3). \quad (4)$$

Studies with simulated samples show that the ratio can be described by a power law as $r_\phi(M_{T2}) = a M_{T2}^b$. The parameters a and b are determined separately in each H_T bin by fitting r_ϕ in an M_{T2} sideband in data after subtracting non-multijet contributions using simulation. The sideband spans M_{T2} values of 60–100 GeV for events with $H_T < 1000$ GeV, and 70–100 GeV for events with larger values of H_T . The fit to the r_ϕ distribution in the $1000 < H_T < 1500$ GeV region is shown in Fig. 3 (left). The inclusive multijet contribution in each signal region, $N_{j,b}^{\text{SR}}(M_{T2})$, is estimated using the ratio $r_\phi(M_{T2})$ measured in the M_{T2} sideband and the number of events in the low- $\Delta\phi_{\min}$ control region, $N_{\text{inc}}^{\text{CR}}(M_{T2})$, according to

$$N_{j,b}^{\text{SR}}(M_{T2}) = N_{\text{inc}}^{\text{CR}}(M_{T2}) r_\phi(M_{T2}) f_j(H_T) r_b(N_j), \quad (5)$$

where f_j is the fraction of multijet events in bin N_j , and r_b is the fraction of events in bin N_j that are in bin N_b . (Here, N_j denotes a jet multiplicity bin, and N_b denotes a b jet multiplicity bin within N_j). The values of f_j and r_b are measured using events with M_{T2} between 100 and 200 GeV in the low $\Delta\phi_{\min}$ sideband, where f_j is measured separately in each H_T bin, while r_b is measured in bins of N_j integrated over H_T , as r_b is found to be independent of the latter. Values of f_j and r_b measured in data are shown in Fig. 3 (center and right) compared to simulation.

The largest uncertainties in the estimate in most regions result from the statistical uncertainty in the fit and from the sensitivity of the r_ϕ value to variations in the fit window. These variations result in an uncertainty that increases with M_{T2} and ranges from 20–50%. The total uncertainty in the estimate is found to be of similar size as in Ref. [6], varying between 40–180% depending on the search region.

An estimate based on $r_\phi(M_{T2})$ is not viable in the monojet search regions, which therefore require a different strategy. A control region is obtained by selecting events with a second jet with $30 < p_T < 60$ GeV and inverting the $\Delta\phi_{\min}$ requirement. After subtracting non-multijet contributions using simulation, the data yield in the control region is taken as an estimate of the background in the corresponding monojet search region. Tests in simulation show the method provides a conservative estimate of the multijet background, which is less than 8% in all monojet search regions. In all monojet bins, a 50% uncertainty in the non-multijet subtraction is combined with the statistical uncertainty from the data yield in the control region with a second jet.

5 Results

The data yields in the search regions are statistically compatible with the estimated backgrounds from SM processes. A summary of the results of this search is shown in Fig. 4. Each bin in the upper panel corresponds to a single H_T , N_j , N_b

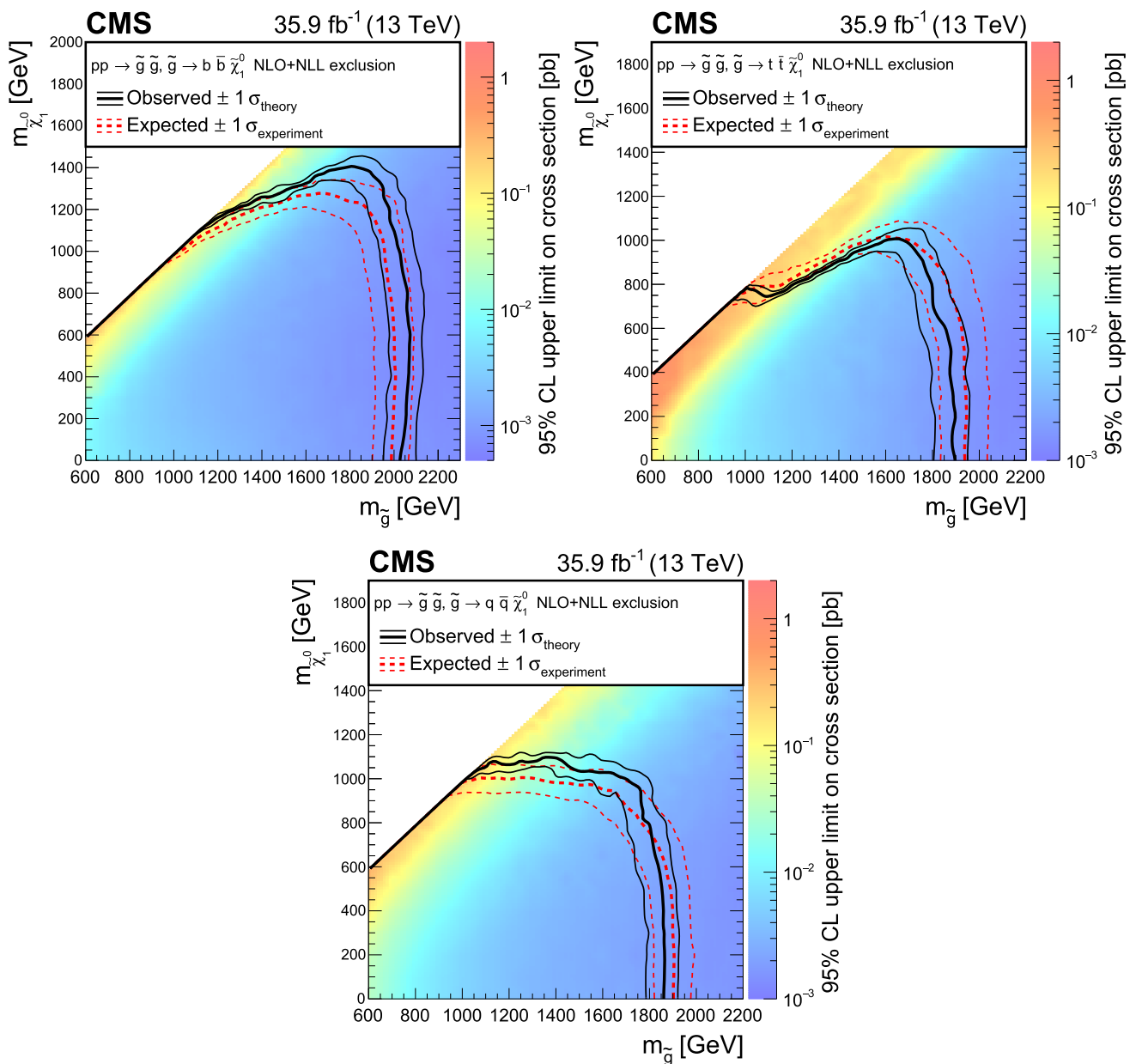


Fig. 6 Exclusion limits at 95% CL for gluino-mediated bottom squark production (upper left), gluino-mediated top squark production (upper right), and gluino-mediated light-flavor (u,d,s,c) squark production (below). The area enclosed by the thick black curve represents the

observed exclusion region, while the dashed red lines indicate the expected limits and their ± 1 standard deviation ranges. The thin black lines show the effect of the theoretical uncertainties on the signal cross section

topological region, integrated over M_{T2} . The lower panel further breaks down the background estimates and observed data yields into M_{T2} bins for the region $575 < H_T < 1000$ GeV. Distributions for the other H_T regions can be found in Appendix B. The background estimates and corresponding uncertainties shown in these plots rely exclusively on the inputs from control samples and simulation described in Sect. 4, and are referred to in the rest of the text as “pre-fit background” results.

To allow simpler reinterpretation, we also provide results for super signal regions, which cover subsets of the full analysis with simpler inclusive selections and that can be used to obtain approximate interpretations of this search. The definitions of these regions are given in Table 2, with the predicted and observed number of events and the 95% confidence level (CL) upper limit on the number of signal events contributing to each region. Limits are set using a modified frequentist approach, employing the CL_s criterion and relying on

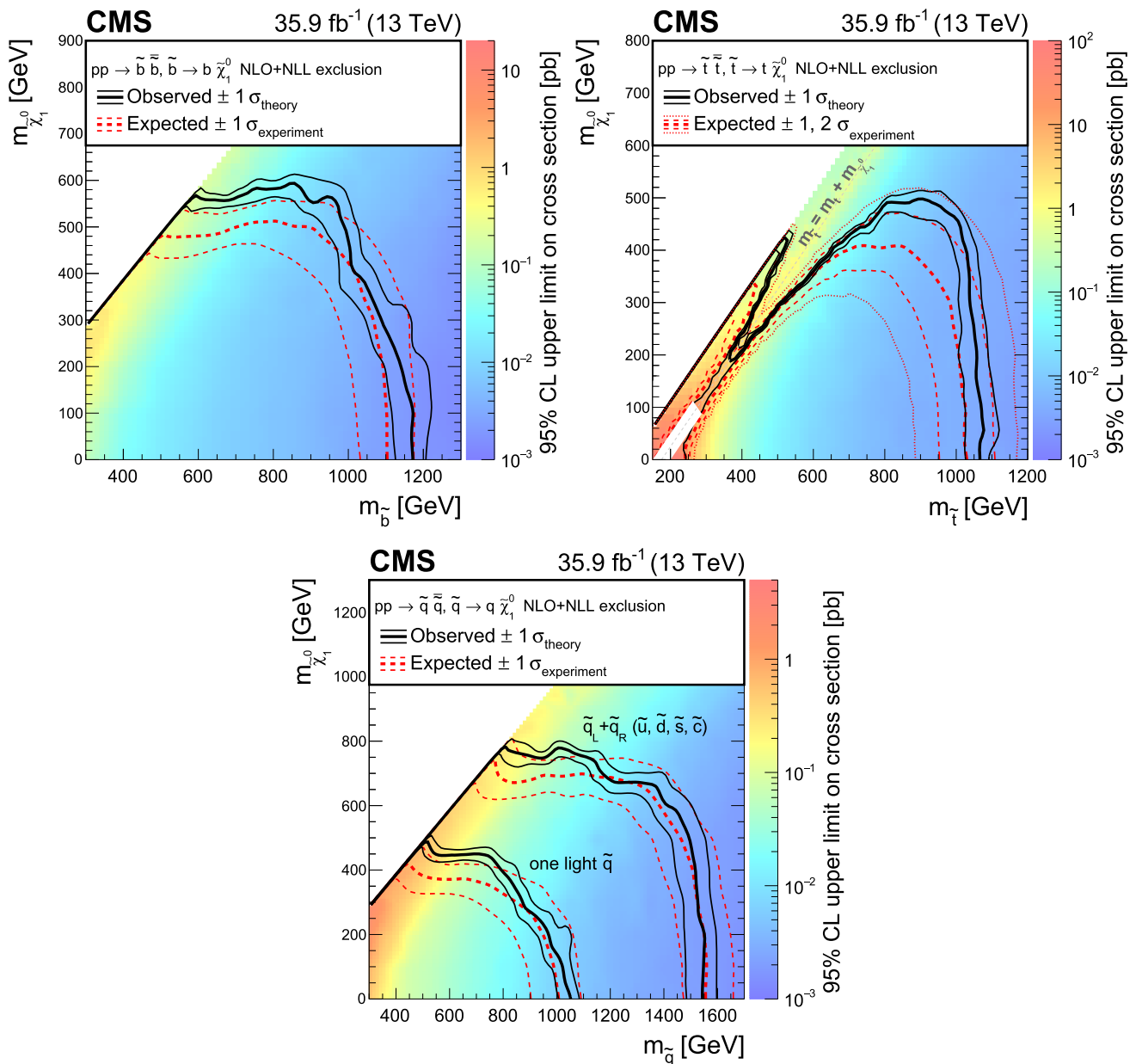


Fig. 7 Exclusion limit at 95% CL for bottom squark pair production (upper left), top squark pair production (upper right), and light-flavor squark pair production (below). The area enclosed by the thick black curve represents the observed exclusion region, while the dashed red lines indicate the expected limits and their ± 1 standard deviation ranges. For the top squark pair production plot, the ± 2 standard deviation ranges are also shown. The thin black lines show the effect of the theoretical

uncertainties on the signal cross section. The white diagonal band in the upper right plot corresponds to the region $|m_{\tilde{t}} - m_t - m_{\tilde{\chi}_1^0}| < 25$ GeV and small $m_{\tilde{\chi}_1^0}$. Here the efficiency of the selection is a strong function of $m_{\tilde{t}} - m_{\tilde{\chi}_1^0}$, and as a result the precise determination of the cross section upper limit is uncertain because of the finite granularity of the available MC samples in this region of the $(m_{\tilde{t}}, m_{\tilde{\chi}_1^0})$ plane

asymptotic approximations to calculate the distribution of the profile likelihood test-statistic used [41–44].

5.1 Interpretation

The results of the search can be interpreted by performing a maximum likelihood fit to the data in the signal

regions. The fit is carried out under either a background-only or a background+signal hypothesis. The uncertainties in the modeling of the backgrounds, summarized in Sect. 4, are inputs to the fitting procedure. The likelihood is constructed as the product of Poisson probability density functions, one for each signal region, with constraint terms that account for uncertainties in the background esti-

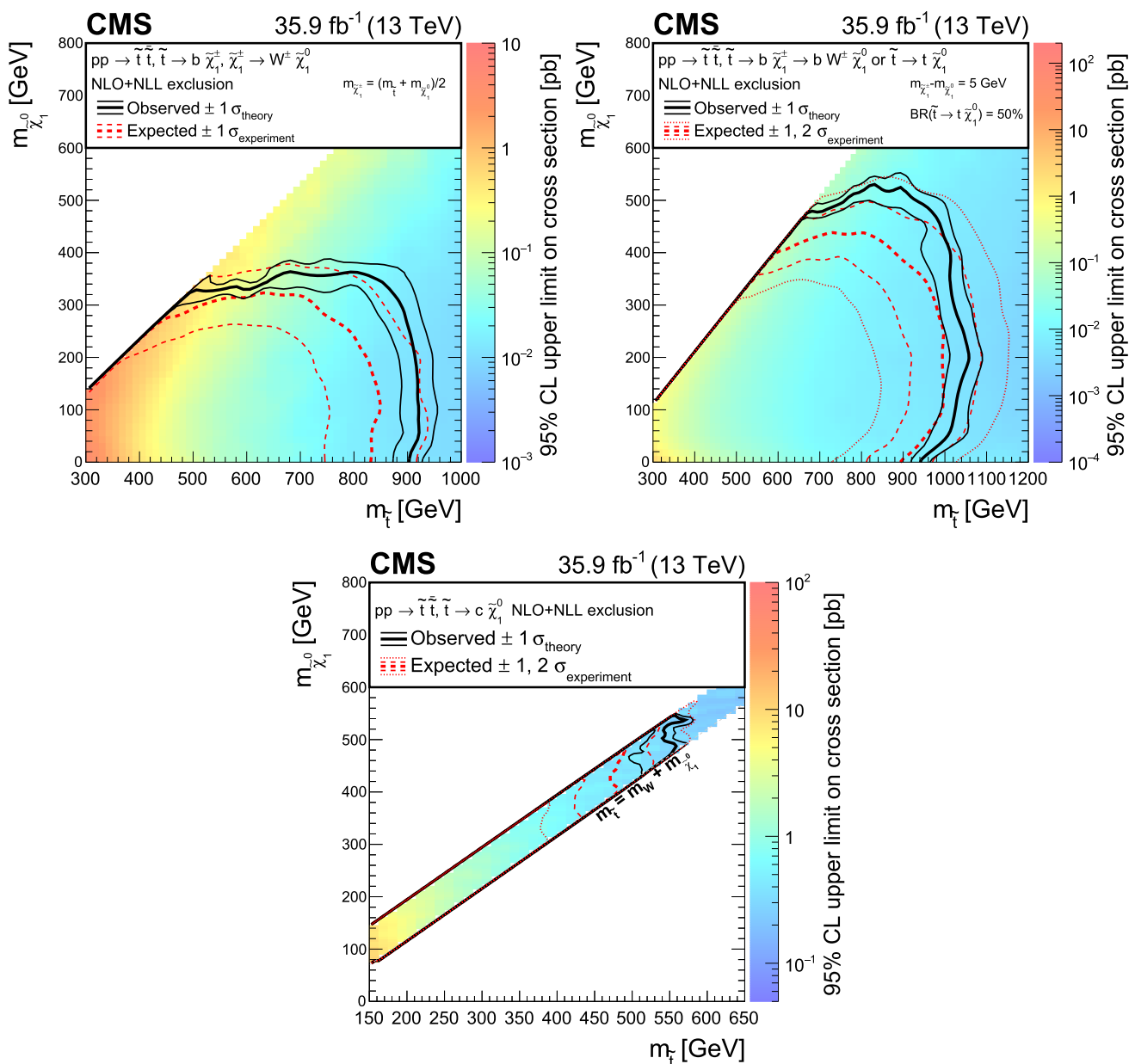


Fig. 8 Exclusion limit at 95% CL for top squark pair production for different decay modes of the top squark. For the scenario where $pp \rightarrow \tilde{t}\tilde{t} \rightarrow b\bar{b}\tilde{\chi}_1^+\tilde{\chi}_1^-, \tilde{\chi}_1^{\pm} \rightarrow W^{\pm}\tilde{\chi}_1^0$ (upper left), the mass of the chargino is chosen to be half way in between the masses of the top squark and the neutralino. A mixed decay scenario (upper right), $pp \rightarrow \tilde{t}\tilde{t} \rightarrow b\bar{b}\tilde{\chi}_1^+\tilde{\chi}_1^0, \tilde{\chi}_1^{\pm} \rightarrow t\tilde{\chi}_1^0$ with equal branching fractions for the top squark decays $t \rightarrow t\tilde{\chi}_1^0$

$\tilde{t} \rightarrow b\tilde{\chi}_1^+, \tilde{\chi}_1^+ \rightarrow W^{*+}\tilde{\chi}_1^0$, is also considered, with the chargino mass chosen such that $\Delta m(\tilde{\chi}_1^{\pm}, \tilde{\chi}_1^0) = 5 \text{ GeV}$. Finally, we also consider a compressed scenario (below) where $pp \rightarrow \tilde{t}\tilde{t} \rightarrow c\bar{c}\tilde{\chi}_1^0\tilde{\chi}_1^0$. The area enclosed by the thick black curve represents the observed exclusion region, while the dashed red lines indicate the expected limits and their ± 1 standard deviation ranges. The thin black lines show the effect of the theoretical uncertainties on the signal cross section

mates and, if considered, the signal yields. The result of the background-only fit, denoted as “post-fit background”, is given in Appendix B. If the magnitude and correlation model of the uncertainties associated to the pre-fit estimates are properly assigned, and the data are found to be in agreement with the estimates, then the fit has the effect of constraining the background and reducing the associated uncertainties.

The results of the search are used to constrain the simplified models of SUSY [45] shown in Fig. 5. For each scenario of gluino (squark) pair production, the simplified models assume that all SUSY particles other than the gluino (squark) and the lightest neutralino are too heavy to be produced directly, and that the gluino (squark) decays promptly. The models assume that each gluino (squark) decays with a 100% branching fraction into the decay products depicted

in Fig. 5. For models where the decays of the two squarks differ, we assume a 50% branching fraction for each decay mode. For the scenario of top squark pair production, the polarization of the top quark is model dependent and is a function of the top-squark and neutralino mixing matrices. To remain agnostic to a particular model realization, events are generated without polarization. Signal cross sections are calculated at NLO+NLL order in α_s [46–50].

Typical values of the uncertainties in the signal yield for the simplified models considered are listed in Table 3. The sources of uncertainties and the methods used to evaluate their effect on the interpretation are the same as those discussed in Ref. [6]. Uncertainties due to the luminosity [51], ISR and pileup modeling, and b tagging and lepton efficiencies are treated as correlated across search bins. Remaining uncertainties are taken as uncorrelated.

Figure 6 shows the exclusion limits at 95% CL for gluino-mediated bottom squark, top squark, and light-flavor squark production. Exclusion limits at 95% CL for the direct production of bottom, top, and light-flavor squark pairs are shown in Fig. 7. Direct production of top squarks for three alternate decay scenarios are also considered, and exclusion limits at 95% CL are shown in Fig. 8. Table 4 summarizes the limits on the masses of the SUSY particles excluded in the simplified model scenarios considered. These results extend the constraints on gluinos and squarks by about 300 GeV and on $\tilde{\chi}_1^0$ by 200 GeV with respect to those in Ref. [6]. The largest differences between the observed and expected limits are found for scenarios of top squark pair production with moderate mass splittings and result from observed yields that are less than the expected background in topological regions with H_T between 575 and 1500 GeV, at least 7 jets, and either one or two b-tagged jets.

We note that the 95% CL upper limits on signal cross sections obtained using the most sensitive super signal regions of Table 2 are typically less stringent by a factor of ~ 1.5 –3 compared to those obtained in the fully-binned analysis. The full analysis performs better because of its larger signal acceptance and because it splits the events into bins with more favorable signal-to-background ratio.

6 Summary

This paper presents the results of a search for new phenomena using events with jets and large M_{T2} . Results are based on a 35.9 fb^{-1} data sample of proton–proton collisions at $\sqrt{s} = 13 \text{ TeV}$ collected in 2016 with the CMS detector. No significant deviations from the standard model expectations are observed. The results are interpreted as limits on the production of new, massive colored particles in simplified models of supersymmetry. This search probes gluino masses up to 2025 GeV and $\tilde{\chi}_1^0$ masses up to 1400 GeV. Constraints

Table 4 Summary of 95% CL observed exclusion limits on the masses of SUSY particles (sparticles) in different simplified model scenarios. The limit on the mass of the produced sparticle is quoted for a massless $\tilde{\chi}_1^0$, while for the mass of the $\tilde{\chi}_1^0$ we quote the highest limit that is obtained

Simplified model	Limit on produced sparticle mass (GeV) for $m_{\tilde{\chi}_1^0} = 0 \text{ GeV}$	Highest limit on the $\tilde{\chi}_1^0$ mass (GeV)
Direct squark production		
Bottom squark	1175	590
Top squark	1070	550
Single light squark	1050	475
Eight degenerate light squarks	1550	775
Gluino-mediated production		
$\tilde{g} \rightarrow b\bar{b}\tilde{\chi}_1^0$	2025	1400
$\tilde{g} \rightarrow t\bar{t}\tilde{\chi}_1^0$	1900	1010
$\tilde{g} \rightarrow q\bar{q}\tilde{\chi}_1^0$	1860	1100

are also obtained on the pair production of light-flavor, bottom, and top squarks, probing masses up to 1550, 1175, and 1070 GeV, respectively, and $\tilde{\chi}_1^0$ masses up to 775, 590, and 550 GeV in each scenario.

Acknowledgements We congratulate our colleagues in the CERN accelerator departments for the excellent performance of the LHC and thank the technical and administrative staffs at CERN and at other CMS institutes for their contributions to the success of the CMS effort. In addition, we gratefully acknowledge the computing centers and personnel of the Worldwide LHC Computing Grid for delivering so effectively the computing infrastructure essential to our analyses. Finally, we acknowledge the enduring support for the construction and operation of the LHC and the CMS detector provided by the following funding agencies: BMFWF and FWF (Austria); FNRS and FWO (Belgium); CNPq, CAPES, FAPERJ, and FAPESP (Brazil); MES (Bulgaria); CERN; CAS, MoST, and NSFC (China); COLCIENCIAS (Colombia); MSES and CSF (Croatia); RPF (Cyprus); SENESCYT (Ecuador); MoER, ERC IUT, and ERDF (Estonia); Academy of Finland, MEC, and HIP (Finland); CEA and CNRS/IN2P3 (France); BMBF, DFG, and HGF (Germany); GSRT (Greece); OTKA and NIH (Hungary); DAE and DST (India); IPM (Iran); SFI (Ireland); INFN (Italy); MSIP and NRF (Republic of Korea); LAS (Lithuania); MOE and UM (Malaysia); BUAP, CINVESTAV, CONACYT, LNS, SEP, and UASLP-FAI (Mexico); MBIE (New Zealand); PAEC (Pakistan); MSHE and NSC (Poland); FCT (Portugal); JINR (Dubna); MON, RosAtom, RAS, RFBR and RAEP (Russia); MESTD (Serbia); SEIDI, CPAN, PCTI and FEDER (Spain); Swiss Funding Agencies (Switzerland); MST (Taipei); ThEPCenter, IPST, STAR, and NSTDA (Thailand); TUBITAK and TAEK (Turkey); NASU and SFFR (Ukraine); STFC (UK); DOE and NSF (USA).

Individuals have received support from the Marie-Curie program and the European Research Council and EPLANET (European Union); the Leventis Foundation; the A. P. Sloan Foundation; the Alexander von Humboldt Foundation; the Belgian Federal Science Policy Office; the Fonds pour la Formation à la Recherche dans l'Industrie et dans l'Agriculture (FRIA-Belgium); the Agentschap voor Innovatie door Wetenschap en Technologie (IWT-Belgium); the Ministry of Education, Youth and Sports (MEYS) of the Czech Republic; the Council of Science and Industrial Research, India; the HOMING PLUS program of the Foun-

dation for Polish Science, cofinanced from European Union, Regional Development Fund, the Mobility Plus program of the Ministry of Science and Higher Education, the National Science Center (Poland), contracts Harmonia 2014/14/M/ST2/00428, Opus 2014/13/B/ST2/02543, 2014/15/B/ST2/03998, and 2015/19/B/ST2/02861, Sonata-bis 2012/07-E/ST2/01406; the National Priorities Research Program by Qatar National Research Fund; the Programa Clarín-COFUND del Principado de Asturias; the Thalís and Aristeia programs cofinanced by EU-ESF and the Greek NSRF; the Rachadapisek Sompot Fund for Post-doctoral Fellowship, Chulalongkorn University and the Chulalongkorn Academic into Its 2nd Century Project Advancement Project (Thailand); and the Welch Foundation, contract C-1845.

Open Access This article is distributed under the terms of the Creative Commons Attribution 4.0 International License (<http://creativecommons.org/licenses/by/4.0/>), which permits unrestricted use, distribution, and reproduction in any medium, provided you give appropriate credit to the original author(s) and the source, provide a link to the Creative Commons license, and indicate if changes were made. Funded by SCOAP³.

A Definition of search regions

The 213 exclusive search regions are defined in Tables 5, 6 and 7.

Table 5 Summary of signal regions for the monojet selection

N_b	Jet p_T binning (GeV)
0	[250, 350, 450, 575, 700, 1000, 1200, ∞)
≥ 1	[250, 350, 450, 575, 700, ∞)

Table 6 The M_{T2} binning in each topological region of the multi-jet search regions, for the very low, low and medium H_T regions

H_T range (GeV)	Jet multiplicities	M_{T2} binning (GeV)	
[250, 450]	2 – 3j, 0b	[200, 300, 400, ∞)	
	2 – 3j, 1b	[200, 300, 400, ∞)	
	2 – 3j, 2b	[200, 300, 400, ∞)	
	$\geq 4j$, 0b	[200, 300, 400, ∞)	
	$\geq 4j$, 1b	[200, 300, 400, ∞)	
	$\geq 4j$, 2b	[200, 300, 400, ∞)	
	$\geq 2j$, $\geq 3b$	[200, 300, 400, ∞)	
	[450, 575]	2 – 3j, 0b	[200, 300, 400, 500, ∞)
		2 – 3j, 1b	[200, 300, 400, 500, ∞)
		2 – 3j, 2b	[200, 300, 400, 500, ∞)
4 – 6j, 0b		[200, 300, 400, 500, ∞)	
4 – 6j, 1b		[200, 300, 400, 500, ∞)	
4 – 6j, 2b		[200, 300, 400, 500, ∞)	
$\geq 7j$, 0b		[200, 300, 400, ∞)	
$\geq 7j$, 1b		[200, 300, 400, ∞)	
$\geq 7j$, 2b		[200, 300, 400, ∞)	
2 – 6j, $\geq 3b$		[200, 300, 400, 500, ∞)	
$\geq 7j$, $\geq 3b$	[200, 300, 400, ∞)		

Table 6 continued

H_T range (GeV)	Jet multiplicities	M_{T2} binning (GeV)
[575, 1000]	2 – 3j, 0b	[200, 300, 400, 600, 800, ∞)
	2 – 3j, 1b	[200, 300, 400, 600, 800, ∞)
	2 – 3j, 2b	[200, 300, 400, 600, 800, ∞)
	4 – 6j, 0b	[200, 300, 400, 600, 800, ∞)
	4 – 6j, 1b	[200, 300, 400, 600, 800, ∞)
	4 – 6j, 2b	[200, 300, 400, 600, 800, ∞)
	$\geq 7j$, 0b	[200, 300, 400, 600, 800, ∞)
	$\geq 7j$, 1b	[200, 300, 400, 600, ∞)
	$\geq 7j$, 2b	[200, 300, 400, 600, ∞)
	2 – 6j, $\geq 3b$	[200, 300, 400, 600, ∞)
	$\geq 7j$, $\geq 3b$	[200, 300, 400, 600, ∞)

Table 7 The M_{T2} binning in each topological region of the multijet search regions, for the high- and extreme- H_T regions

H_T range (GeV)	Jet multiplicities	M_{T2} binning (GeV)
[1000, 1500]	2 – 3j, 0b	[200, 400, 600, 800, 1000, 1200, ∞)
	2 – 3j, 1b	[200, 400, 600, 800, 1000, 1200, ∞)
	2 – 3j, 2b	[200, 400, 600, 800, 1000, ∞)
	4 – 6j, 0b	[200, 400, 600, 800, 1000, 1200, ∞)
	4 – 6j, 1b	[200, 400, 600, 800, 1000, 1200, ∞)
	4 – 6j, 2b	[200, 400, 600, 800, 1000, ∞)
	$\geq 7j$, 0b	[200, 400, 600, 800, 1000, ∞)
	$\geq 7j$, 1b	[200, 400, 600, 800, ∞)
	$\geq 7j$, 2b	[200, 400, 600, 800, ∞)
	2 – 6j, $\geq 3b$	[200, 400, 600, ∞)
	$\geq 7j$, $\geq 3b$	[200, 400, 600, ∞)
	[1500, ∞)	2 – 3j, 0b
2 – 3j, 1b		[400, 600, 800, 1000, ∞)
2 – 3j, 2b		[400, ∞)
4 – 6j, 0b		[400, 600, 800, 1000, 1400, ∞)
4 – 6j, 1b		[400, 600, 800, 1000, 1400, ∞)
4 – 6j, 2b		[400, 600, 800, ∞)
$\geq 7j$, 0b		[400, 600, 800, 1000, ∞)
$\geq 7j$, 1b		[400, 600, 800, ∞)
$\geq 7j$, 2b		[400, 600, 800, ∞)
2 – 6j, $\geq 3b$		[400, 600, ∞)
$\geq 7j$, $\geq 3b$		[400, ∞)

B Detailed results

See Figs. 9, 10, 11, 12, 13 and 14 in Appendix.

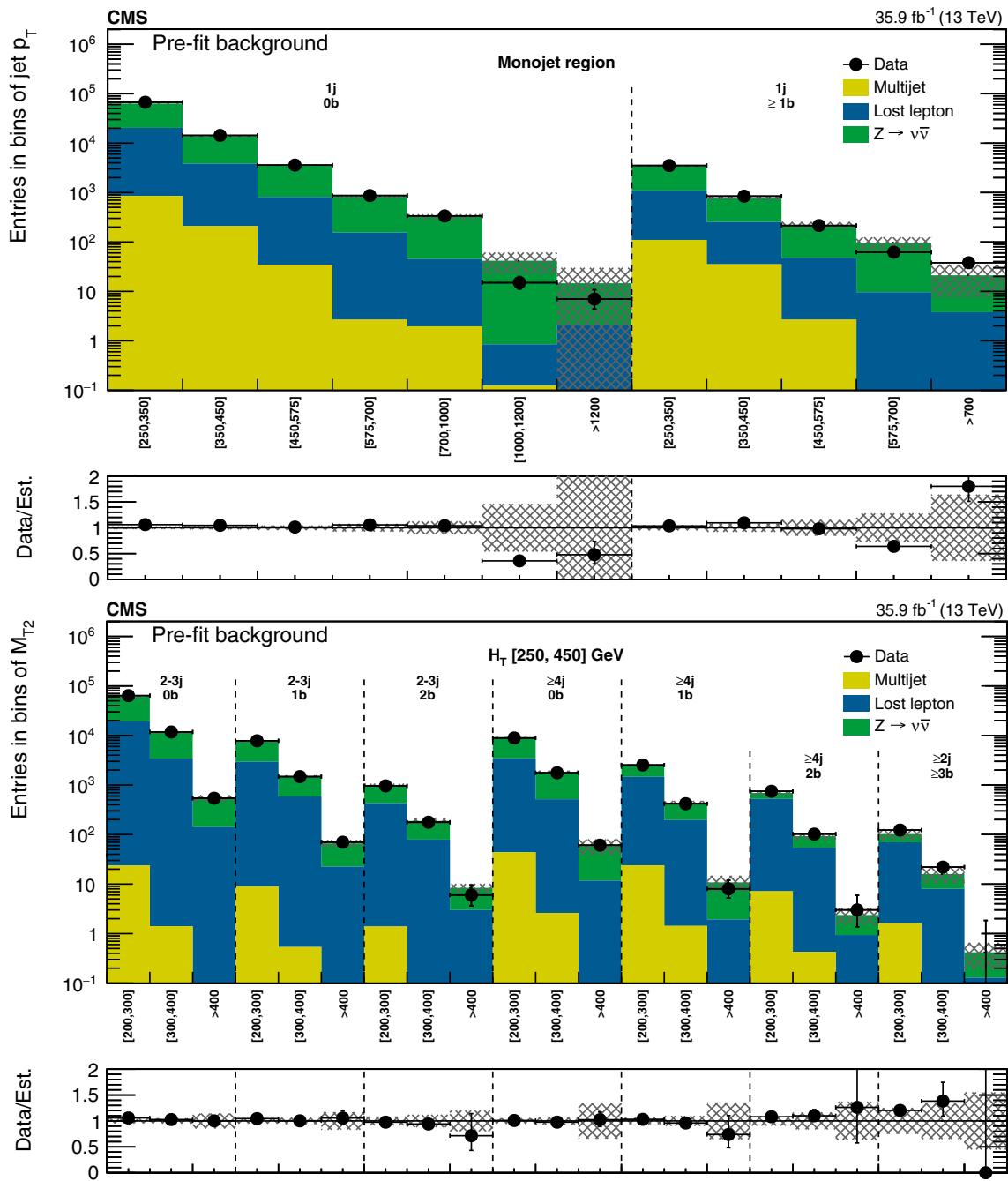
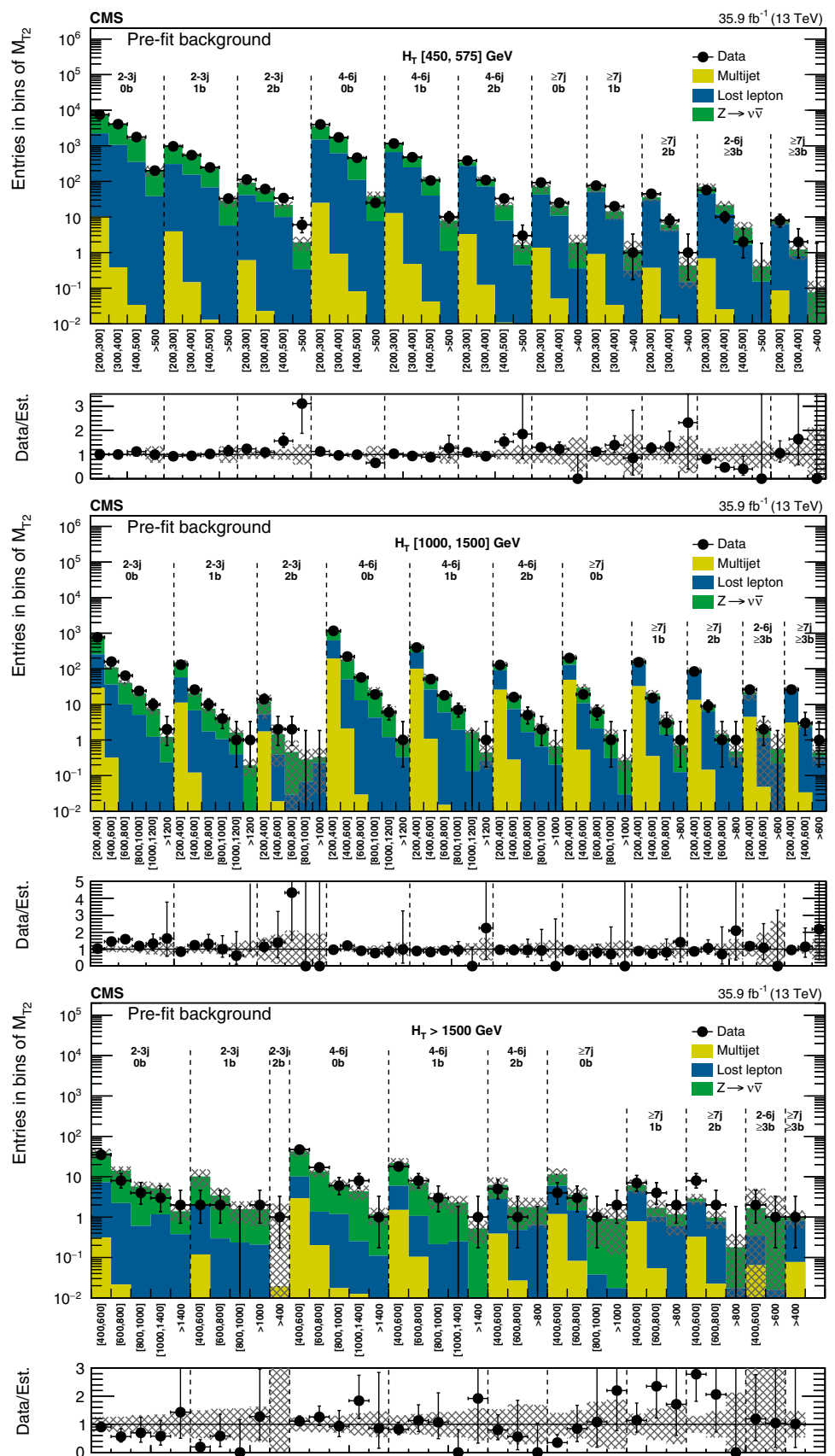


Fig. 9 (Upper) Comparison of the estimated background and observed data events in each signal bin in the monojet region. On the x -axis, the p_T^{jet1} binning is shown in units of GeV. Hatched bands represent the full

uncertainty in the background estimate. (Lower) Same for the very low H_T region. On the x -axis, the M_{T2} binning is shown in units of GeV

Fig. 10 (Upper) Comparison of the estimated background and observed data events in each signal bin in the low- H_T region. Hatched bands represent the full uncertainty in the background estimate. Same for the high- (middle) and extreme- (lower) H_T regions. On the x -axis, the M_{T2} binning is shown in units of GeV. For the extreme- H_T region, the last bin is left empty for visualization purposes



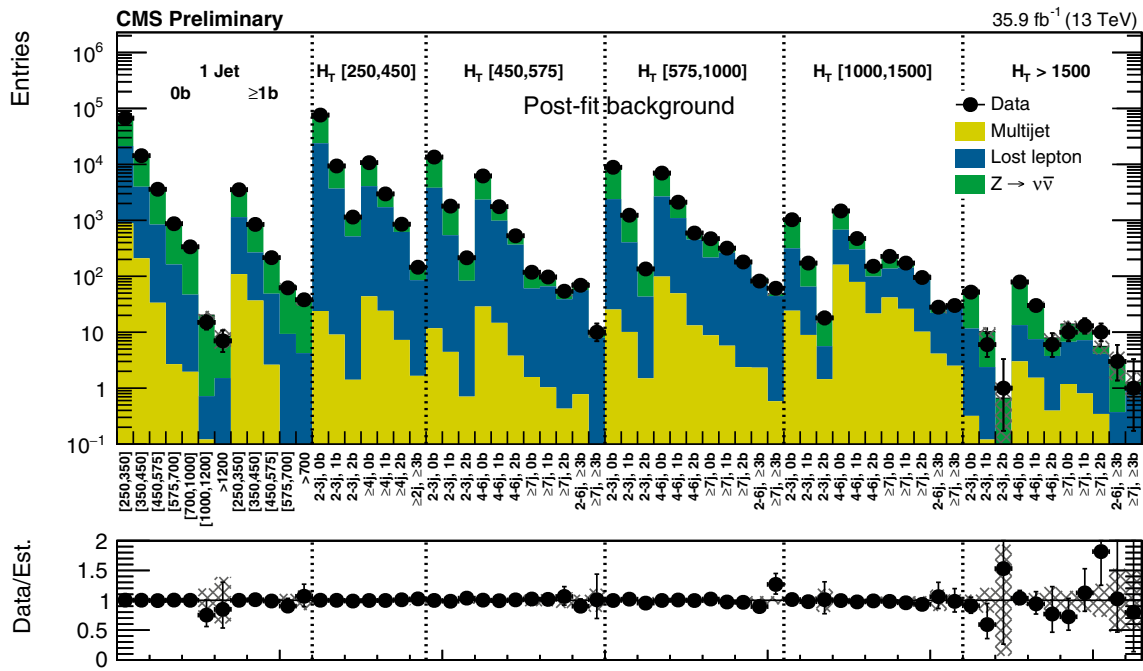


Fig. 11 Comparison of post-fit background prediction and observed data events in each topological region. Hatched bands represent the post-fit uncertainty in the background prediction. For the monojet, on

the x-axis the p_T^{jet1} binning is shown in units of GeV, whereas for the multijet signal regions, the notations j, b indicate N_j , N_b labeling

Fig. 12 (Upper) Comparison of the post-fit background prediction and observed data events in each signal bin in the monojet region. On the x -axis, the p_T^{jet} binning is shown in units of GeV. (Middle) and (lower): Same for the very low and low- H_T region. On the x -axis, the M_{T2} binning is shown in units of GeV. The hatched bands represent the post-fit uncertainty in the background prediction

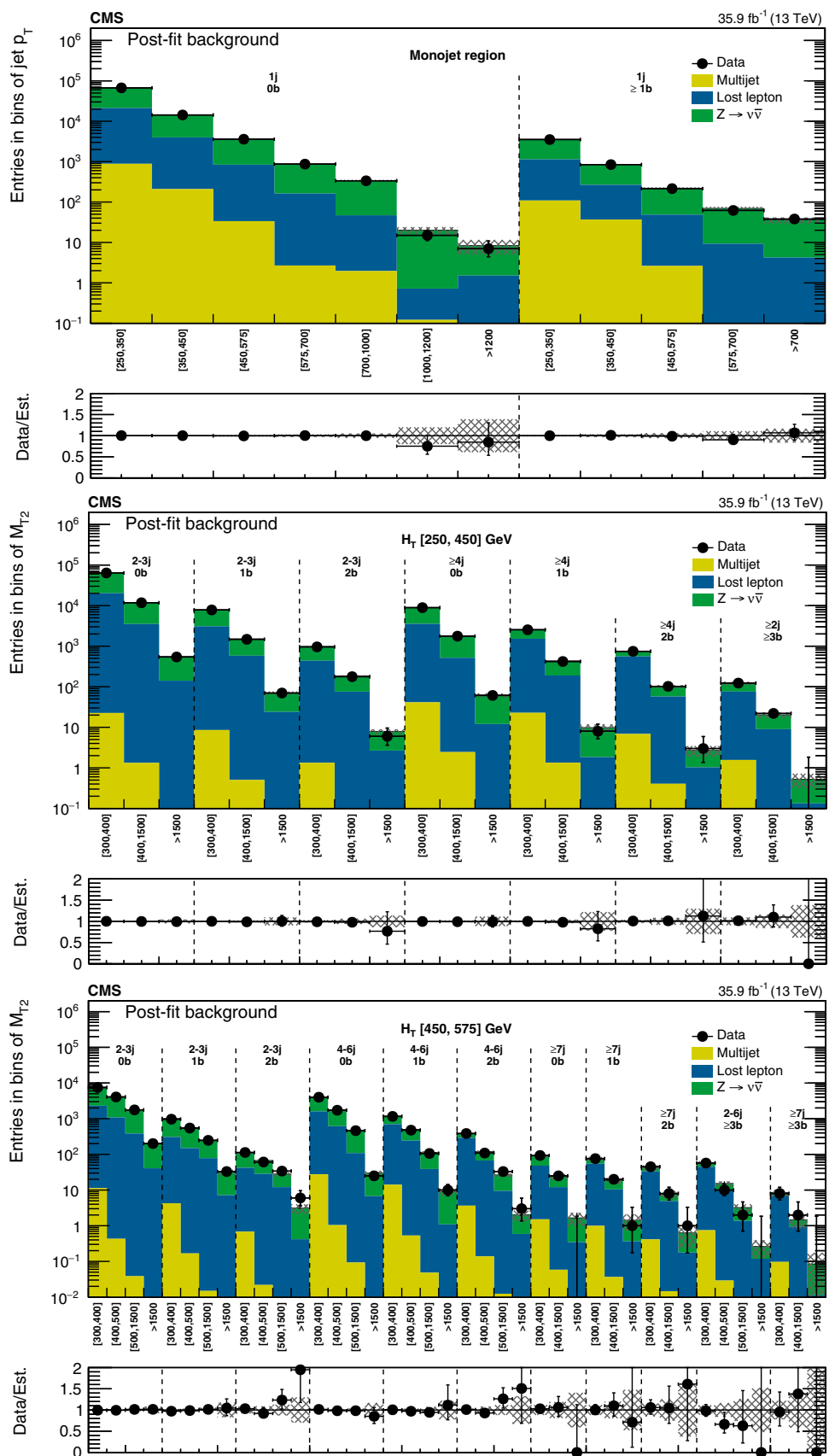
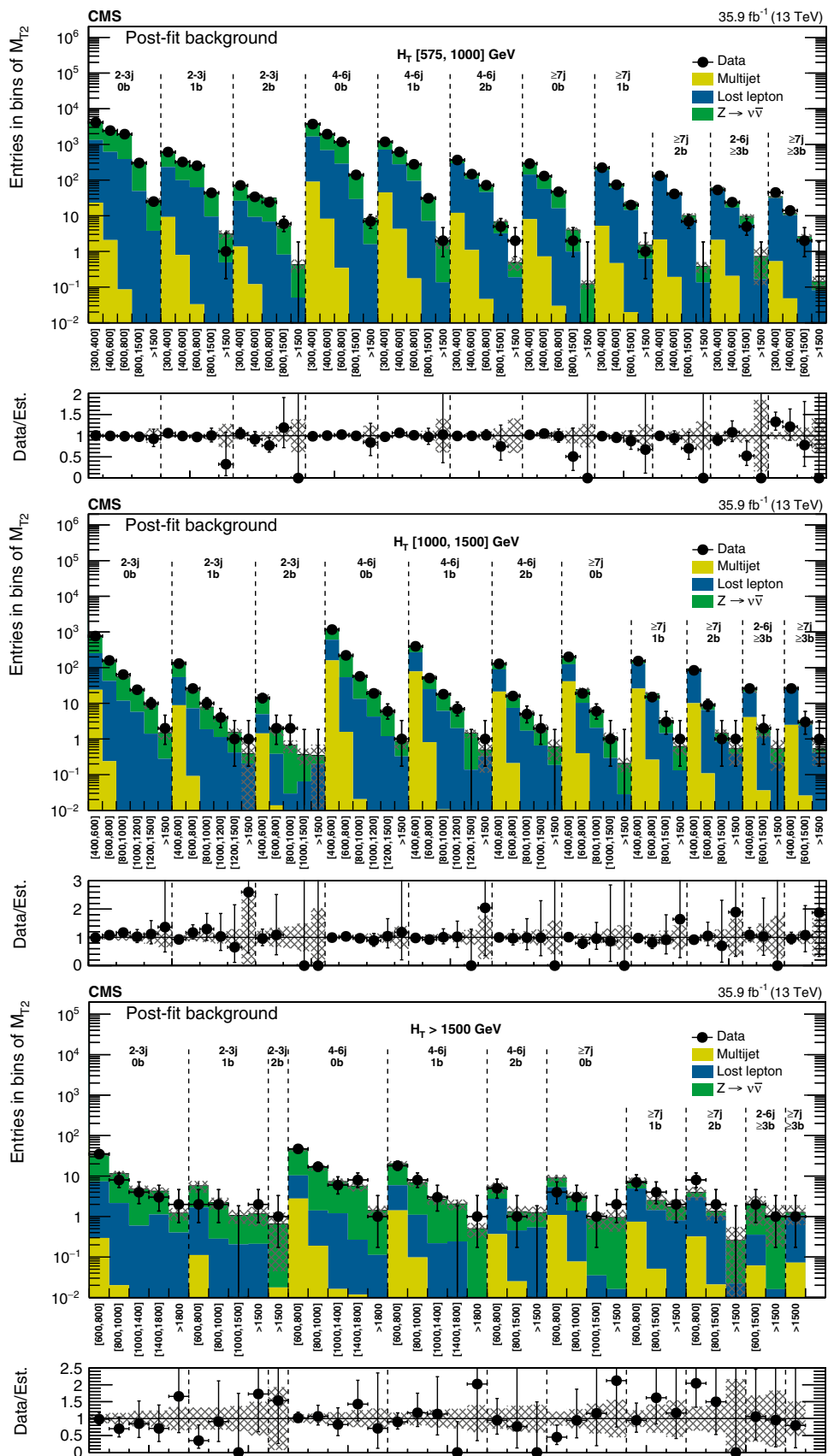


Fig. 13 (Upper) Comparison of the post-fit background prediction and observed data events in each signal bin in the medium- H_T region. Same for the high- (middle) and extreme- (lower) H_T regions. On the x -axis, the M_{T2} binning is shown in units of GeV. The hatched bands represent the post-fit uncertainty in the background prediction. For the extreme- H_T region, the last bin is left empty for visualization purposes



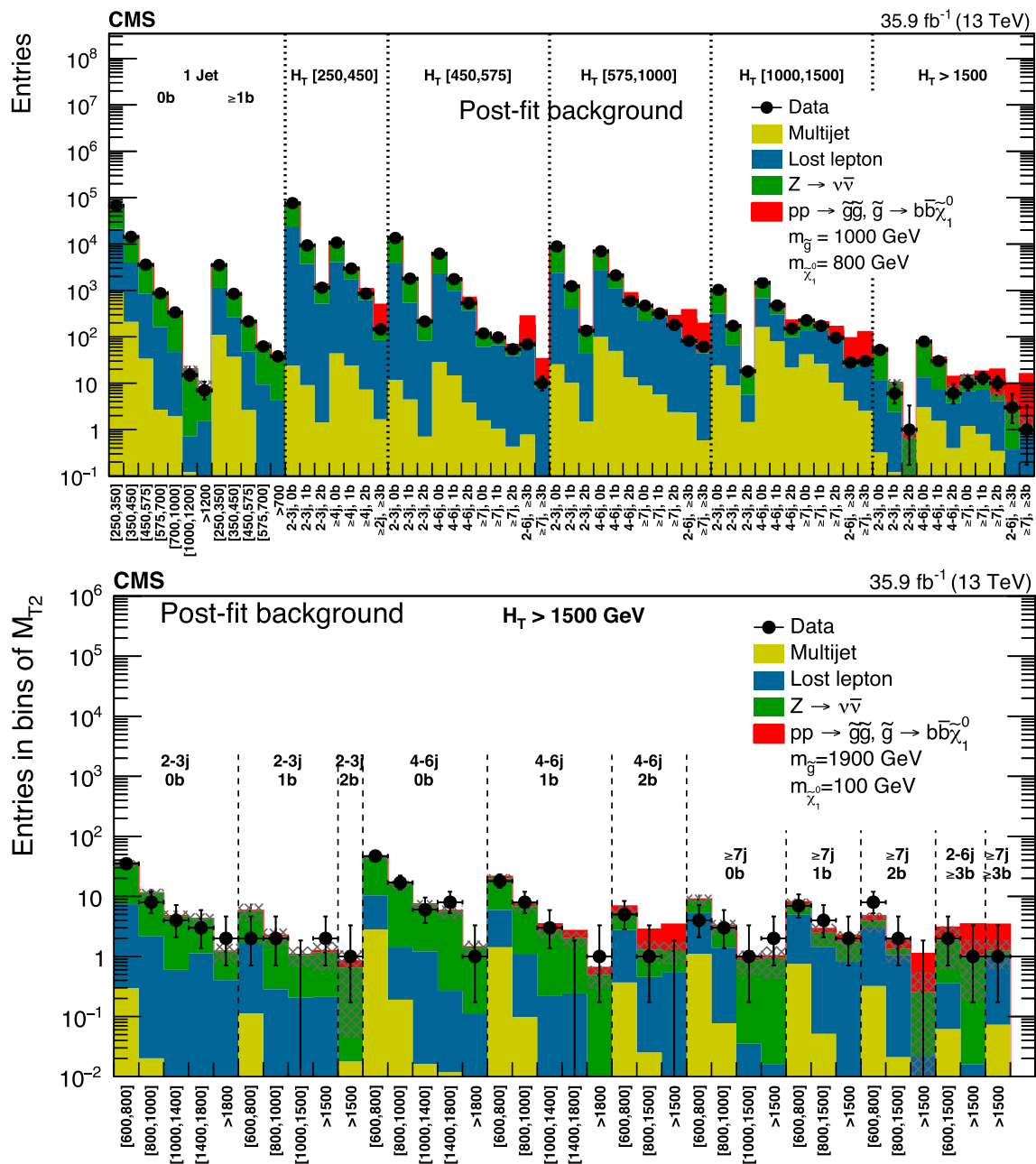


Fig. 14 (Upper) The post-fit background prediction and observed data events in the analysis binning, for all topological regions with the expected yield for the signal model of gluino mediated bottom-squark production ($m_{\tilde{g}} = 1000$ GeV, $m_{\tilde{\chi}_1^0} = 800$ GeV) stacked on top of the expected background. For the monojet regions, the p_T^{jet1} binning is in

units of GeV. (Lower) Same for the extreme- H_T region for the same signal with ($m_{\tilde{g}} = 1900$ GeV, $m_{\tilde{\chi}_1^0} = 100$ GeV). On the x-axis, the M_{T2} binning is shown in units of GeV. The hatched bands represent the post-fit uncertainty in the background prediction. For the extreme- H_T region, the last bin is left empty for visualization purposes

References

1. ATLAS Collaboration, Search for new phenomena in final states with large jet multiplicities and missing transverse momentum with ATLAS using $\sqrt{s} = 13$ TeV proton–proton collisions. Phys. Lett. B **757**, 334 (2016). doi:10.1016/j.physletb.2016.04.005. arXiv:1602.06194

2. ATLAS Collaboration, Search for new phenomena in final states with an energetic jet and large missing transverse momentum in pp collisions at $\sqrt{s} = 13$ TeV using the ATLAS detector. Phys. Rev. D **94**, 032005 (2016). doi:10.1103/PhysRevD.94.032005. arXiv:1604.07773
3. ATLAS Collaboration, Search for squarks and gluinos in final states with jets and missing transverse momentum at $\sqrt{s} = 13$ TeV with

- the ATLAS detector. *Eur. Phys. J. C* **76**, 392 (2016). doi:10.1140/epjc/s10052-016-4184-8. arXiv:1605.03814
4. ATLAS Collaboration, Search for pair production of gluinos decaying via stop and sbottom in events with b -jets and large missing transverse momentum in pp collisions at $\sqrt{s} = 13$ TeV with the ATLAS detector. *Phys. Rev. D* **94**, 032003 (2016). doi:10.1103/PhysRevD.94.032003. arXiv:1605.09318
 5. ATLAS Collaboration, Search for bottom squark pair production in proton–proton collisions at $\sqrt{s} = 13$ TeV with the ATLAS detector. *Eur. Phys. J. C* **76**, 547 (2016). doi:10.1140/epjc/s10052-016-4382-4. arXiv:1606.08772
 6. CMS Collaboration, Search for new physics with the M_{T2} variable in all-jets final states produced in pp collisions at $\sqrt{s} = 13$ TeV. *JHEP* **10**, 006 (2016). doi:10.1007/JHEP10(2016)006. arXiv:1603.04053
 7. CMS Collaboration, Search for supersymmetry in the multijet and missing transverse momentum final state in pp collisions at 13 TeV. *Phys. Lett. B* **758**, 152 (2016). doi:10.1016/j.physletb.2016.05.002. arXiv:1602.06581
 8. CMS Collaboration, Inclusive search for supersymmetry using razor variables in pp collisions at $\sqrt{s} = 13$ TeV. *Phys. Rev. D* **95**, 012003 (2017). doi:10.1103/PhysRevD.95.012003. arXiv:1609.07658
 9. CMS Collaboration, A search for new phenomena in pp collisions at $\sqrt{s} = 13$ TeV in final states with missing transverse momentum and at least one jet using the α_T variable (2016). arXiv:1611.00338. Submitted to: *Eur. Phys. J. C*
 10. C.G. Lester, D.J. Summers, Measuring masses of semiinvisibly decaying particles pair produced at hadron colliders. *Phys. Lett. B* **463**, 99 (1999). doi:10.1016/S0370-2693(99)00945-4. arXiv:hep-ph/9906349
 11. P. Ramond, Dual theory for free fermions. *Phys. Rev. D* **3**, 2415 (1971). doi:10.1103/PhysRevD.3.2415
 12. Y.A. Golfand, E.P. Likhman, Extension of the algebra of Poincaré group generators and violation of P invariance. *JETP Lett.* **13**, 323 (1971). http://www.jetpletters.ac.ru/ps/1584/article_24309.pdf
 13. A. Neveu, J.H. Schwarz, Factorizable dual model of pions. *Nucl. Phys. B* **31**, 86 (1971). doi:10.1016/0550-3213(71)90448-2
 14. D.V. Volkov, V.P. Akulov, Possible universal neutrino interaction. *JETP Lett.* **16**, 438 (1972). http://www.jetpletters.ac.ru/ps/1766/article_26864.pdf
 15. J. Wess, B. Zumino, A Lagrangian model invariant under supergauge transformations. *Phys. Lett. B* **49**, 52 (1974). doi:10.1016/0370-2693(74)90578-4
 16. J. Wess, B. Zumino, Supergauge transformations in four dimensions. *Nucl. Phys. B* **70**, 39 (1974). doi:10.1016/0550-3213(74)90355-1
 17. P. Fayet, Supergauge invariant extension of the Higgs mechanism and a model for the electron and its neutrino. *Nucl. Phys. B* **90**, 104 (1975). doi:10.1016/0550-3213(75)90636-7
 18. H.P. Nilles, Supersymmetry, supergravity and particle physics. *Phys. Rep.* **110**, 1 (1984). doi:10.1016/0370-1573(84)90008-5
 19. C.M.S. Collaboration, The CMS experiment at the CERN LHC. *JINST* **3**, S08004 (2008). doi:10.1088/1748-0221/3/08/S08004
 20. CMS Collaboration, The CMS trigger system. *JINST* **12**(01), P01020 (2017). doi:10.1088/1748-0221/12/01/P01020. arXiv:1609.02366
 21. CMS Collaboration, Particle-flow reconstruction and global event description with the CMS detector (2017). arXiv:1706.04965. Submitted to *JINST*
 22. M. Cacciari, G.P. Salam, G. Soyez, The anti- k_t jet clustering algorithm. *JHEP* **04**, 063 (2008). doi:10.1088/1126-6708/2008/04/063. arXiv:0802.1189
 23. M. Cacciari, G.P. Salam, G. Soyez, FastJet user manual. *Eur. Phys. J. C* **72**, 1896 (2012). doi:10.1140/epjc/s10052-012-1896-2. arXiv:1111.6097
 24. M. Cacciari, G.P. Salam, Pileup subtraction using jet areas. *Phys. Lett. B* **659**, 119 (2008). doi:10.1016/j.physletb.2007.09.077. arXiv:0707.1378
 25. CMS Collaboration, Identification of b quark jets at the CMS Experiment in the LHC Run 2. CMS Physics Analysis Summary CMS-PAS-BTV-15-001, CERN (2016). <https://cds.cern.ch/record/2138504>
 26. C.M.S. Collaboration, Missing transverse energy performance of the CMS detector. *JINST* **6**, P09001 (2011). doi:10.1088/1748-0221/6/09/P09001. arXiv:1106.5048
 27. CMS Collaboration, Performance of missing energy reconstruction in 13 TeV pp collision data using the CMS detector. CMS Physics Analysis Summary CMS-PAS-JME-16-004, CERN (2016). <https://cds.cern.ch/record/2205284>
 28. T. Sjöstrand, The Lund Monte Carlo for e^+e^- jet physics. *Comput. Phys. Commun.* **28**, 229 (1983). doi:10.1016/0010-4655(83)90041-3
 29. T. Sjöstrand, S. Mrenna, P. Skands, PYTHIA 6.4 physics and manual., *JHEP* **05**, 026 (2006). doi:10.1088/1126-6708/2006/05/026. arXiv:hep-ph/0603175
 30. J. Alwall et al., The automated computation of tree-level and next-to-leading order differential cross sections, and their matching to parton shower simulations. *JHEP* **07**, 079 (2014). doi:10.1007/JHEP07(2014)079. arXiv:1405.0301
 31. J. Alwall et al., Comparative study of various algorithms for the merging of parton showers and matrix elements in hadronic collisions. *Eur. Phys. J. C* **53**, 473 (2008). doi:10.1140/epjc/s10052-007-0490-5. arXiv:0706.2569
 32. T. Sjöstrand, S. Mrenna, P. Skands, A brief introduction to PYTHIA 8.1. *Comput. Phys. Commun.* **178**, 852 (2008). doi:10.1016/j.cpc.2008.01.036. arXiv:0710.3820
 33. S. Alioli, P. Nason, C. Oleari, E. Re, NLO single-top production matched with shower in POWHEG: s - and t -channel contributions. *JHEP* **09**, 111 (2009). doi:10.1088/1126-6708/2009/09/111. arXiv:0907.4076. [Erratum: doi:10.1007/JHEP02(2010)011]
 34. E. Re, Single-top Wt -channel production matched with parton showers using the POWHEG method. *Eur. Phys. J. C* **71**, 1547 (2011). doi:10.1140/epjc/s10052-011-1547-z. arXiv:1009.2450
 35. Nucl. Instrum. Methods A GEANT4-a simulation toolkit. **506**, 250 (2003). doi:10.1016/S0168-9002(03)01368-8
 36. S. Abdullin et al., The fast simulation of the CMS detector at LHC. *J. Phys. Conf. Ser.* **331**, 032049 (2011). doi:10.1088/1742-6596/331/3/032049
 37. R. Gavin, Y. Li, F. Petriello, S. Quackenbush, FEWZ 2.0: a code for hadronic Z production at next-to-next-to-leading order. *Comput. Phys. Commun.* **182**, 2388 (2011). doi:10.1016/j.cpc.2011.06.008. arXiv:1011.3540
 38. R. Gavin, Y. Li, F. Petriello, S. Quackenbush, W physics at the LHC with FEWZ 2.1. *Comput. Phys. Commun.* **184**, 208 (2013). doi:10.1016/j.cpc.2012.09.005. arXiv:1201.5896
 39. M. Czakon, A. Mitov, Top++: a program for the calculation of the top-pair cross-section at hadron colliders. *Comput. Phys. Commun.* **185**, 2930 (2014). doi:10.1016/j.cpc.2014.06.021. arXiv:1112.5675
 40. C. Borschensky et al., Squark and gluino production cross sections in pp collisions at $\sqrt{s} = 13, 14, 33$ and 100 TeV. *Eur. Phys. J. C* **74**, 3174 (2014). doi:10.1140/epjc/s10052-014-3174-y. arXiv:1407.5066
 41. A.L. Read, Presentation of search results: the CL_s technique. *J. Phys. G* **28**, 2693 (2002). doi:10.1088/0954-3899/28/10/313
 42. T. Junk, Confidence level computation for combining searches with small statistics. *Nucl. Instrum. Methods A* **434**, 435 (1999). doi:10.1016/S0168-9002(99)00498-2. arXiv:hep-ex/9902006
 43. G. Cowan, K. Cranmer, E. Gross, O. Vitells, Asymptotic formulae for likelihood-based tests of new physics. *Eur. Phys. J. C* **71**, 1554

44. ATLAS and CMS Collaboration, Procedure for the LHC Higgs boson search combination in summer 2011. ATLAS/CMS joint note ATL-PHYS-PUB-2011-011, CMS-NOTE-2011-005, CERN (2011). <http://cds.cern.ch/record/1379837>
45. CMS Collaboration, Interpretation of searches for supersymmetry with simplified models. *Phys. Rev. D* **88**(5), 052017 (2013). doi:10.1103/PhysRevD.88.052017. arXiv:1301.2175
46. W. Beenakker, R. Höpker, M. Spira, P.M. Zerwas, Squark and gluino production at hadron colliders. *Nucl. Phys. B* **492**, 51 (1997). doi:10.1016/S0550-3213(97)00084-9. arXiv:hep-ph/9610490
47. A. Kulesza, L. Motyka, Threshold resummation for squark-antisquark and gluino-pair production at the LHC. *Phys. Rev. Lett.* **102**, 111802 (2009). doi:10.1103/PhysRevLett.102.111802. arXiv:0807.2405
48. A. Kulesza, L. Motyka, Soft gluon resummation for the production of gluino–gluino and squark–antisquark pairs at the LHC. *Phys. Rev. D* **80**, 095004 (2009). doi:10.1103/PhysRevD.80.095004. arXiv:0905.4749
49. W. Beenakker et al., Soft-gluon resummation for squark and gluino hadroproduction. *JHEP* **12**, 041 (2009). doi:10.1088/1126-6708/2009/12/041. arXiv:0909.4418
50. W. Beenakker et al., Squark and gluino hadroproduction. *Int. J. Mod. Phys. A* **26**, 2637 (2011). doi:10.1142/S0217751X11053560. arXiv:1105.1110
51. CMS Collaboration, CMS luminosity measurements for the 2016 data taking period. CMS Physics Analysis Summary CMS-PAS-LUM-17-001, CERN (2017). <https://cds.cern.ch/record/2257069>

CMS Collaboration

Yerevan Physics Institute, Yerevan, Armenia

A. M. Sirunyan, A. Tumasyan, A. Johnson⁴¹

Institut für Hochenergiephysik, Wien, Austria

W. Adam, F. Ambrogio, E. Asilar, T. Bergauer, J. Brandstetter, E. Brondolin, M. Dragicevic, J. Erö, M. Flechl, M. Friedl, R. Frühwirth¹, V. M. Ghete, J. Grossmann, J. Hrubec, M. Jeitler¹, A. König, N. Krammer, I. Krätschmer, D. Liko, T. Madlener, I. Mikulec, E. Pree, D. Rabady, N. Rad, H. Rohringer, J. Schieck¹, R. Schöfbeck, M. Spanring, D. Spitzbart, J. Strauss, W. Waltenberger, J. Wittmann, C.-E. Wulz¹, M. Zarucki

Institute for Nuclear Problems, Minsk, Belarus

V. Chekhovsky, V. Mossolov, J. Suarez Gonzalez

Universiteit Antwerpen, Antwerp, Belgium

E. A. De Wolf, D. Di Croce, X. Janssen, J. Lauwers, M. Van De Klundert, H. Van Haevermaet, P. Van Mechelen, N. Van Remortel, A. Van Spilbeeck

Vrije Universiteit Brussel, Brussels, Belgium

S. Abu Zeid, F. Blekman, J. D'Hondt, I. De Bruyn, J. De Clercq, K. Deroover, G. Flouris, D. Lontkovskyi, S. Lowette, S. Moortgat, L. Moreels, A. Olbrechts, Q. Python, K. Skovpen, S. Tavernier, W. Van Doninck, P. Van Mulders, I. Van Parijs

Université Libre de Bruxelles, Brussels, Belgium

H. Brun, B. Clerbaux, G. De Lentdecker, H. Delannoy, G. Fasanella, L. Favart, R. Goldouzian, A. Grebenyuk, G. Karapostoli, T. Lenzi, J. Luetic, T. Maerschalk, A. Marinov, A. Randle-conde, T. Seva, C. Vander Velde, P. Vanlaer, D. Vannerom, R. Yonamine, F. Zenoni, F. Zhang²

Ghent University, Ghent, Belgium

A. Cimmino, T. Cornelis, D. Dobur, A. Fagot, M. Gul, I. Khvastunov, D. Poyraz, C. Roskas, S. Salva, M. Tytgat, W. Verbeke, N. Zaganidis

Université Catholique de Louvain, Louvain-la-Neuve, Belgium

H. Bakhshiansohi, O. Bondu, S. Brochet, G. Bruno, A. Caudron, S. De Visscher, C. Delaere, M. Delcourt, B. Francois, A. Giammanco, A. Jafari, M. Komm, G. Krintiras, V. Lemaitre, A. Magitteri, A. Mertens, M. Musich, K. Piotrkowski, L. Quertenmont, M. Vidal Marono, S. Wertz

Université de Mons, Mons, Belgium

N. Belyi

Centro Brasileiro de Pesquisas Fisicas, Rio de Janeiro, Brazil

W. L. Aldá Júnior, F. L. Alves, G. A. Alves, L. Brito, M. Correa Martins Junior, C. Hensel, A. Moraes, M. E. Pol, P. Rebello Teles

Universidade do Estado do Rio de Janeiro, Rio de Janeiro, Brazil

E. Belchior Batista Das Chagas, W. Carvalho, J. Chinellato³, A. Custódio, E. M. Da Costa, G. G. Da Silveira⁴, D. De Jesus Damiao, S. Fonseca De Souza, L. M. Huertas Guativa, H. Malbouisson, M. Melo De Almeida, C. Mora Herrera, L. Mundim, H. Nogima, A. Santoro, A. Sznajder, E. J. Tonelli Manganote³, F. Torres Da Silva De Araujo, A. Vilela Pereira

Universidade Estadual Paulista^a, Universidade Federal do ABC^b, São Paulo, Brazil

S. Ahuja^a, C. A. Bernardes^a, T. R. Fernandez Perez Tomei^a, E. M. Gregores^b, P. G. Mercadante^b, C. S. Moon^a, S. F. Novaes^a, Sandra S. Padula^a, D. Romero Abad^b, J. C. Ruiz Vargas^a

Institute for Nuclear Research and Nuclear Energy of Bulgaria Academy of Sciences, Sofia, Bulgaria

A. Aleksandrov, R. Hadjiiska, P. Iaydjiev, M. Misheva, M. Rodozov, M. Shopova, S. Stoykova, G. Sultanov

University of Sofia, Sofia, Bulgaria

A. Dimitrov, I. Glushkov, L. Litov, B. Pavlov, P. Petkov

Beihang University, Beijing, China

W. Fang⁵, X. Gao⁵

Institute of High Energy Physics, Beijing, China

M. Ahmad, J. G. Bian, G. M. Chen, H. S. Chen, M. Chen, Y. Chen, C. H. Jiang, D. Leggat, Z. Liu, F. Romeo, S. M. Shaheen, A. Spiezia, J. Tao, C. Wang, Z. Wang, E. Yazgan, H. Zhang, J. Zhao

State Key Laboratory of Nuclear Physics and Technology, Peking University, Beijing, China

Y. Ban, G. Chen, Q. Li, S. Liu, Y. Mao, S. J. Qian, D. Wang, Z. Xu

Universidad de Los Andes, Bogota, Colombia

C. Avila, A. Cabrera, L. F. Chaparro Sierra, C. Florez, C. F. González Hernández, J. D. Ruiz Alvarez

Faculty of Electrical Engineering, Mechanical Engineering and Naval Architecture, University of Split, Split, Croatia

B. Courbon, N. Godinovic, D. Lelas, I. Puljak, P. M. Ribeiro Cipriano, T. Sculac

Faculty of Science, University of Split, Split, Croatia

Z. Antunovic, M. Kovac

Institute Rudjer Boskovic, Zagreb, Croatia

V. Brigljevic, D. Ferencek, K. Kadija, B. Mesic, T. Susa

University of Cyprus, Nicosia, Cyprus

M. W. Ather, A. Attikis, G. Mavromanolakis, J. Mousa, C. Nicolaou, F. Ptochos, P. A. Razis, H. Rykaczewski

Charles University, Prague, Czech Republic

M. Finger⁶, M. Finger Jr.⁶

Universidad San Francisco de Quito, Quito, Ecuador

E. Carrera Jarrin

Academy of Scientific Research and Technology of the Arab Republic of Egypt, Egyptian Network of High Energy Physics, Cairo, Egypt

A. Ellithi Kamel⁷, S. Khalil⁸, A. Mohamed⁸

National Institute of Chemical Physics and Biophysics, Tallinn, Estonia

R. K. Dewanjee, M. Kadastik, L. Perrini, M. Raidal, A. Tiko, C. Veelken

Department of Physics, University of Helsinki, Helsinki, Finland

P. Eerola, J. Pekkanen, M. Voutilainen

Helsinki Institute of Physics, Helsinki, Finland

J. Härkönen, T. Järvinen, V. Karimäki, R. Kinnunen, T. Lampén, K. Lassila-Perini, S. Lehti, T. Lindén, P. Luukka, E. Tuominen, J. Tuominiemi, E. Tuovinen

Lappeenranta University of Technology, Lappeenranta, Finland

J. Talvitie, T. Tuuva

IRFU, CEA, Université Paris-Saclay, Gif-sur-Yvette, France

M. Besancon, F. Couderc, M. Dejardin, D. Denegri, J. L. Faure, F. Ferri, S. Ganjour, S. Ghosh, A. Givernaud, P. Gras, G. Hamel de Monchenault, P. Jarry, I. Kucher, E. Locci, M. Machet, J. Malcles, G. Negro, J. Rander, A. Rosowsky, M. Ö. Sahin, M. Titov

Laboratoire Leprince-Ringuet, Ecole Polytechnique, CNRS/IN2P3, Université Paris-Saclay, Palaiseau, France

A. Abdulsalam, I. Antropov, S. Baffioni, F. Beaudette, P. Busson, L. Cadamuro, E. Chapon, C. Charlot, O. Davignon, R. Granier de Cassagnac, M. Jo, S. Lisniak, A. Lobanov, J. Martin Blanco, M. Nguyen, C. Ochando, G. Ortona, P. Paganini, P. Pigard, S. Regnard, R. Salerno, J. B. Sauvan, Y. Sirois, A. G. Stahl Leiton, T. Strebler, Y. Yilmaz, A. Zabi

Université de Strasbourg, CNRS, IPHC UMR 7178, 67000 Strasbourg, FranceJ.-L. Agram⁹, J. Andrea, A. Aubin, J.-M. Brom, M. Buttignol, E. C. Chabert, N. Chanon, C. Collard, E. Conte⁹, X. Coubez, J.-C. Fontaine⁹, D. Gelé, U. Goerlach, M. Jansová, A.-C. Le Bihan, N. Tonon, P. Van Hove**Centre de Calcul de l'Institut National de Physique Nucleaire et de Physique des Particules, CNRS/IN2P3, Villeurbanne, France**

S. Gadrat

Université de Lyon, Université Claude Bernard Lyon 1, CNRS-IN2P3, Institut de Physique Nucléaire de Lyon, Villeurbanne, FranceS. Beauceron, C. Bernet, G. Boudoul, R. Chierici, D. Contardo, P. Depasse, H. El Mamouni, J. Fay, L. Finco, S. Gascon, M. Gouzevitch, G. Grenier, B. Ille, F. Lagarde, I. B. Laktineh, M. Lethuillier, L. Mirabito, A. L. Pequegnot, S. Perries, A. Popov¹⁰, V. Sordini, M. Vander Donckt, S. Viret**Georgian Technical University, Tbilisi, Georgia**A. Khvedelidze⁶**Tbilisi State University, Tbilisi, Georgia**Z. Tsamalaidze⁶**RWTH Aachen University, I. Physikalisches Institut, Aachen, Germany**

C. Autermann, S. Beranek, L. Feld, M. K. Kiesel, K. Klein, M. Lipinski, M. Preuten, C. Schomakers, J. Schulz, T. Verlage

RWTH Aachen University, III. Physikalisches Institut A, Aachen, Germany

A. Albert, M. Brodski, E. Dietz-Laursonn, D. Duchardt, M. Endres, M. Erdmann, S. Erdweg, T. Esch, R. Fischer, A. Güth, M. Hamer, T. Hebbeker, C. Heidemann, K. Hoepfner, S. Knutzen, M. Merschmeyer, A. Meyer, P. Millet, S. Mukherjee, M. Olschewski, K. Padeken, T. Pook, M. Radziej, H. Reithler, M. Rieger, F. Scheuch, D. Teysier, S. Thüer

RWTH Aachen University, III. Physikalisches Institut B, Aachen, GermanyG. Flügge, B. Kargoll, T. Kress, A. Künsken, J. Lingemann, T. Müller, A. Nehr Korn, A. Nowack, C. Pistone, O. Pooth, A. Stahl¹¹**Deutsches Elektronen-Synchrotron, Hamburg, Germany**M. Aldaya Martin, T. Arndt, C. Asawatangtrakuldee, K. Beernaert, O. Behnke, U. Behrens, A. A. Bin Anuar, K. Borrás¹², V. Botta, A. Campbell, P. Connor, C. Contreras-Campana, F. Costanza, C. Diez Pardos, G. Eckerlin, D. Eckstein, T. Eichhorn, E. Eren, E. Gallo¹³, J. Garay Garcia, A. Geiser, A. Gizhko, J. M. Grados Luyando, A. Grohsjean, P. Gunnellini, A. Harb, J. Hauk, M. Hempel¹⁴, H. Jung, A. Kalogeropoulos, M. Kasemann, J. Keaveney, C. Kleinwort, I. Korol, D. Krücker, W. Lange, A. Lelek, T. Lenz, J. Leonard, K. Lipka, W. Lohmann¹⁴, R. Mankel, I.-A. Melzer-Pellmann, A. B. Meyer, G. Mittag, J. Mnich, A. Mussgiller, E. Ntomari, D. Pitzl, R. Placakyte, A. Raspereza, B. Roland, M. Savitskyi, P. Saxena, R. Shevchenko, S. Spannagel, N. Stefaniuk, G. P. Van Onsem, R. Walsh, Y. Wen, K. Wichmann, C. Wissing, O. Zenaiev

University of Hamburg, Hamburg, Germany

S. Bein, V. Blobel, M. Centis Vignali, A. R. Draeger, T. Dreyer, E. Garutti, D. Gonzalez, J. Haller, A. Hinzmann, M. Hoffmann, A. Junkes, A. Karavdina, R. Klanner, R. Kogler, N. Kovalchuk, S. Kurz, T. Lapsien, I. Marchesini, D. Marconi, M. Meyer, M. Niedziela, D. Nowatschin, F. Pantaleo¹¹, T. Peiffer, A. Perieanu, C. Scharf, P. Schleper, A. Schmidt, S. Schumann, J. Schwandt, J. Sonneveld, H. Stadie, G. Steinbrück, F. M. Stober, M. Stöver, H. Tholen, D. Troendle, E. Usai, L. Vanelderen, A. Vanhoefer, B. Vormwald

Institut für Experimentelle Kernphysik, Karlsruhe, Germany

M. Akbiyik, C. Barth, S. Baur, E. Butz, R. Caspart, T. Chwalek, F. Colombo, W. De Boer, A. Dierlamm, B. Freund, R. Friese, M. Giffels, A. Gilbert, D. Haitz, F. Hartmann¹¹, S. M. Heindl, U. Husemann, F. Kassel¹¹, S. Kudella, H. Mildner, M. U. Mozer, Th. Müller, M. Plagge, G. Quast, K. Rabbertz, M. Schröder, I. Shvetsov, G. Sieber, H. J. Simonis, R. Ulrich, S. Wayand, M. Weber, T. Weiler, S. Williamson, C. Wöhrmann, R. Wolf

Institute of Nuclear and Particle Physics (INPP), NCSR Demokritos, Aghia Paraskevi, Greece

G. Anagnostou, G. Daskalakis, T. Geralis, V. A. Giakoumopoulou, A. Kyriakis, D. Loukas, I. Topsis-Giotis

National and Kapodistrian University of Athens, Athens, Greece

S. Kesisoglou, A. Panagiotou, N. Saoulidou

University of Ioánnina, Ioánnina, Greece

I. Evangelou, C. Foudas, P. Kokkas, N. Manthos, I. Papadopoulos, E. Paradas, J. Strologas, F. A. Triantis

MTA-ELTE Lendület CMS Particle and Nuclear Physics Group, Eötvös Loránd University, Budapest, Hungary

M. Csanad, N. Filipovic, G. Pasztor

Wigner Research Centre for Physics, Budapest, Hungary

G. Bencze, C. Hajdu, D. Horvath¹⁵, Á. Hunyadi, F. Sikler, V. Veszpremi, G. Vesztergombi¹⁶, A. J. Zsigmond

Institute of Nuclear Research ATOMKI, Debrecen, Hungary

N. Beni, S. Czellar, J. Karancsi¹⁷, A. Makovec, J. Molnar, Z. Szillasi

Institute of Physics, University of Debrecen, Debrecen, Hungary

M. Bartók¹⁶, P. Raics, Z. L. Trocsanyi, B. Ujvari

Indian Institute of Science (IISc), Bangalore, India

S. Choudhury, J. R. Komaragiri

National Institute of Science Education and Research, Bhubaneswar, India

S. Bahinipati¹⁸, S. Bhowmik, P. Mal, K. Mandal, A. Nayak¹⁹, D. K. Sahoo¹⁸, N. Sahoo, S. K. Swain

Panjab University, Chandigarh, India

S. Bansal, S. B. Beri, V. Bhatnagar, U. Bhawandeep, R. Chawla, N. Dhingra, A. K. Kalsi, A. Kaur, M. Kaur, R. Kumar, P. Kumari, A. Mehta, J. B. Singh, G. Walia

University of Delhi, Delhi, India

Ashok Kumar, Aashaq Shah, A. Bhardwaj, S. Chauhan, B. C. Choudhary, R. B. Garg, S. Keshri, A. Kumar, S. Malhotra, M. Naimuddin, K. Ranjan, R. Sharma, V. Sharma

Saha Institute of Nuclear Physics, HBNI, Kolkata, India

R. Bhardwaj, R. Bhattacharya, S. Bhattacharya, S. Dey, S. Dutt, S. Dutt, S. Ghosh, N. Majumdar, A. Modak, K. Mondal, S. Mukhopadhyay, S. Nandan, A. Purohit, A. Roy, D. Roy, S. Roy Chowdhury, S. Sarkar, M. Sharan, S. Thakur

Indian Institute of Technology Madras, Chennai, India

P. K. Behera

Bhabha Atomic Research Centre, Mumbai, India

R. Chudasama, D. Dutta, V. Jha, V. Kumar, A. K. Mohanty¹¹, P. K. Netrakanti, L. M. Pant, P. Shukla, A. Topkar

Tata Institute of Fundamental Research-A, Mumbai, India

T. Aziz, S. Dugad, B. Mahakud, S. Mitra, G. B. Mohanty, B. Parida, N. Sur, B. Sutar

Tata Institute of Fundamental Research-B, Mumbai, India

S. Banerjee, S. Bhattacharya, S. Chatterjee, P. Das, M. Guchait, Sa. Jain, S. Kumar, M. Maity²⁰, G. Majumder, K. Mazumdar, T. Sarkar²⁰, N. Wickramage²¹

Indian Institute of Science Education and Research (IISER), Pune, India

S. Chauhan, S. Dube, V. Hegde, A. Kapoor, K. Kothekar, S. Pandey, A. Rane, S. Sharma

Institute for Research in Fundamental Sciences (IPM), Tehran, Iran

S. Chenarani²², E. Eskandari Tadavani, S. M. Etesami²², M. Khakzad, M. Mohammadi Najafabadi, M. Naseri, S. Paktinat Mehdiabadi²³, F. Rezaei Hosseinabadi, B. Safarzadeh²⁴, M. Zeinali

University College Dublin, Dublin, Ireland

M. Felcini, M. Grunewald

INFN Sezione di Bari^a, Università di Bari^b, Politecnico di Bari^c, Bari, Italy

M. Abbrescia^{a,b}, C. Calabria^{a,b}, C. Caputo^{a,b}, A. Colaleo^a, D. Creanza^{a,c}, L. Cristella^{a,b}, N. De Filippis^{a,c}, M. De Palma^{a,b}, F. Errico^{a,b}, S. Lezki^{a,b}, L. Fiore^a, G. Iaselli^{a,c}, G. Maggi^{a,c}, M. Maggi^a, G. Miniello^{a,b}, S. My^{a,b}, S. Nuzzo^{a,b}, A. Pompili^{a,b}, G. Pugliese^{a,c}, R. Radogna^{a,b}, A. Ranieri^a, G. Selvaggi^{a,b}, A. Sharma^a, L. Silvestris^{a,11}, R. Venditti^a, P. Verwilligen^a

INFN Sezione di Bologna^a, Università di Bologna^b, Bologna, Italy

G. Abbiendi^a, C. Battilana, D. Bonacorsi^{a,b}, S. Braibant-Giacomelli^{a,b}, L. Brigliadori^{a,b}, R. Campanini^{a,b}, P. Capiluppi^{a,b}, A. Castro^{a,b}, F. R. Cavallo^a, S. S. Chhibra^{a,b}, G. Codispoti^{a,b}, M. Cuffiani^{a,b}, G. M. Dallavalle^a, F. Fabbri^a, A. Fanfani^{a,b}, D. Fasanella^{a,b}, P. Giacomelli^a, L. Guiducci^{a,b}, S. Marcellini^a, G. Masetti^a, F. L. Navarria^{a,b}, A. Perrotta^a, A. M. Rossi^{a,b}, T. Rovelli^{a,b}, G. P. Siroli^{a,b}, N. Tosi^{a,b,11}

INFN Sezione di Catania^a, Università di Catania^b, Catania, Italy

S. Albergo^{a,b}, S. Costa^{a,b}, A. Di Mattia^a, F. Giordano^{a,b}, R. Potenza^{a,b}, A. Tricomi^{a,b}, C. Tuve^{a,b}

INFN Sezione di Firenze^a, Università di Firenze^b, Firenze, Italy

G. Barbagli^a, K. Chatterjee^{a,b}, V. Ciulli^{a,b}, C. Civinini^a, R. D'Alessandro^{a,b}, E. Focardi^{a,b}, P. Lenzi^{a,b}, M. Meschini^a, S. Paoletti^a, L. Russo^{a,25}, G. Sguazzoni^a, D. Strom^a, L. Viliani^{a,b,11}

INFN Laboratori Nazionali di Frascati, Frascati, Italy

L. Benussi, S. Bianco, F. Fabbri, D. Piccolo, F. Primavera¹¹

INFN Sezione di Genova^a, Università di Genova^b, Genova, Italy

V. Calvelli^{a,b}, F. Ferro^a, E. Robutti^a, S. Tosi^{a,b}

INFN Sezione di Milano-Bicocca^a, Università di Milano-Bicocca^b, Milan, Italy

L. Brianza^{a,b}, F. Brivio^{a,b}, V. Ciriolo^{a,b}, M. E. Dinardo^{a,b}, S. Fiorendi^{a,b}, S. Gennai^a, A. Ghezzi^{a,b}, P. Govoni^{a,b}, M. Malberti^{a,b}, S. Malvezzi^a, R. A. Manzoni^{a,b}, D. Menasce^a, L. Moroni^a, M. Paganoni^{a,b}, K. Pauwels^{a,b}, D. Pedrini^a, S. Pigazzini^{a,b,26}, S. Ragazzi^{a,b}, T. Tabarelli de Fatis^{a,b}

INFN Sezione di Napoli^a, Università di Napoli 'Federico II'^b, Naples, Italy, Università della Basilicata^c, Potenza, Italy, Università G. Marconi^d, Rome, Italy

S. Buontempo^a, N. Cavallo^{a,c}, S. Di Guida^{a,d,11}, M. Esposito^{a,b}, F. Fabozzi^{a,c}, F. Fienga^{a,b}, A. O. M. Iorio^{a,b}, W. A. Khan^a, G. Lanza^a, L. Lista^a, S. Meola^{a,d,11}, P. Paolucci^{a,11}, C. Sciacca^{a,b}, F. Thyssen^a

INFN Sezione di Padova^a, Università di Padova^b, Padua, Italy, Università di Trento^c, Trento, Italy

P. Azzi^{a,11}, N. Bacchetta^a, L. Benato^{a,b}, M. Biasotto^{a,27}, D. Bisello^{a,b}, A. Boletti^{a,b}, R. Carlin^{a,b}, A. Carvalho Antunes De Oliveira^{a,b}, P. Checchia^a, M. Dall'Osso^{a,b}, P. De Castro Manzano^a, T. Dorigo^a, U. Dosselli^a, S. Fantinel^a, F. Fanzago^a, U. Gasparini^{a,b}, S. Lacaprara^a, M. Margoni^{a,b}, A. T. Meneguzzo^{a,b}, N. Pozzobon^{a,b}, P. Ronchese^{a,b}, R. Rossin^{a,b}, F. Simonetto^{a,b}, E. Torassa^a, M. Zanetti^{a,b}, P. Zotto^{a,b}

INFN Sezione di Pavia^a, Università di Pavia^b, Pavia, Italy

A. Braghieri^a, F. Fallavollita^{a,b}, A. Magnani^{a,b}, P. Montagna^{a,b}, S. P. Ratti^{a,b}, V. Re^a, M. Ressegotti, C. Riccardi^{a,b}, P. Salvini^a, I. Vai^{a,b}, P. Vitulo^{a,b}

INFN Sezione di Perugia^a, Università di Perugia^b, Perugia, Italy

L. Alunni Solestizi^{a,b}, G. M. Bilei^a, D. Ciangottini^{a,b}, L. Fanò^{a,b}, P. Lariccia^{a,b}, R. Leonardi^{a,b}, G. Mantovani^{a,b}, V. Mariani^{a,b}, M. Menichelli^a, A. Saha^a, A. Santocchia^{a,b}, D. Spiga

INFN Sezione di Pisa^a, Università di Pisa^b, Scuola Normale Superiore di Pisa^c, Pisa, Italy

K. Androsova^a, P. Azzurri^{a,11}, G. Bagliesi^a, J. Bernardini^a, T. Boccali^a, L. Borrello, R. Castaldi^a, M. A. Ciocci^{a,b}, R. Dell'Orso^a, G. Fedi^a, L. Giannini^{a,c}, A. Giassi^a, M. T. Grippo^{a,25}, F. Ligabue^{a,c}, T. Lomtadze^a, E. Manca^{a,c}, G. Mandorli^{a,c}, L. Martini^{a,b}, A. Messineo^{a,b}, F. Palla^a, A. Rizzi^{a,b}, A. Savoy-Navarro^{a,28}, P. Spagnolo^a, R. Tenchini^a, G. Tonelli^{a,b}, A. Venturi^a, P. G. Verdini^a

INFN Sezione di Roma^a, Sapienza Università di Roma^b, Rome, Italy

L. Barone^{a,b}, F. Cavallari^a, M. Cipriani^{a,b}, D. Del Re^{a,b,11}, M. Diemoz^a, S. Gelli^{a,b}, E. Longo^{a,b}, F. Margaroli^{a,b}, B. Marzocchi^{a,b}, P. Meridiani^a, G. Organtini^{a,b}, R. Paramatti^{a,b}, F. Preiato^{a,b}, S. Rahatlou^{a,b}, C. Rovelli^a, F. Santanastasio^{a,b}

INFN Sezione di Torino^a, Università di Torino^b, Turin, Italy, Università del Piemonte Orientale^c, Novara, Italy

N. Amapane^{a,b}, R. Arcidiacono^{a,c,11}, S. Argiro^{a,b}, M. Arneodo^{a,c}, N. Bartosik^a, R. Bellan^{a,b}, C. Biino^a, N. Cartiglia^a, F. Cenna^{a,b}, M. Costa^{a,b}, R. Covarelli^{a,b}, A. Degano^{a,b}, N. Demaria^a, B. Kiani^{a,b}, C. Mariotti^a, S. Maselli^a, E. Migliore^{a,b}, V. Monaco^{a,b}, E. Monteil^{a,b}, M. Monteno^a, M. M. Obertino^{a,b}, L. Pacher^{a,b}, N. Pastrone^a, M. Pelliccioni^a, G. L. Pinna Angioni^{a,b}, F. Ravera^{a,b}, A. Romero^{a,b}, M. Ruspa^{a,c}, R. Sacchi^{a,b}, K. Shchelina^{a,b}, V. Sola^a, A. Solano^{a,b}, A. Staiano^a, P. Traczyk^{a,b}

INFN Sezione di Trieste^a, Università di Trieste^b, Trieste, Italy

S. Belforte^a, M. Casarsa^a, F. Cossutti^a, G. Della Ricca^{a,b}, A. Zanetti^a

Kyungpook National University, Daegu, Korea

D. H. Kim, G. N. Kim, M. S. Kim, J. Lee, S. Lee, S. W. Lee, Y. D. Oh, S. Sekmen, D. C. Son, Y. C. Yang

Chonbuk National University, Jeonju, Korea

A. Lee

Institute for Universe and Elementary Particles, Chonnam National University, Kwangju, Korea

H. Kim, D. H. Moon, G. Oh

Hanyang University, Seoul, Korea

J. A. Brochero Cifuentes, J. Goh, T. J. Kim

Korea University, Seoul, Korea

S. Cho, S. Choi, Y. Go, D. Gyun, S. Ha, B. Hong, Y. Jo, Y. Kim, K. Lee, K. S. Lee, S. Lee, J. Lim, S. K. Park, Y. Roh

Seoul National University, Seoul, Korea

J. Almond, J. Kim, J. S. Kim, H. Lee, K. Lee, K. Nam, S. B. Oh, B. C. Radburn-Smith, S. h. Seo, U. K. Yang, H. D. Yoo, G. B. Yu

University of Seoul, Seoul, Korea

M. Choi, H. Kim, J. H. Kim, J. S. H. Lee, I. C. Park, G. Ryu

Sungkyunkwan University, Suwon, Korea

Y. Choi, C. Hwang, J. Lee, I. Yu

Vilnius University, Vilnius, Lithuania

V. Dudenias, A. Juodagalvis, J. Vaitkus

National Centre for Particle Physics, Universiti Malaya, Kuala Lumpur, Malaysia

I. Ahmed, Z. A. Ibrahim, M. A. B. Md Ali²⁹, F. Mohamad Idris³⁰, W. A. T. Wan Abdullah, M. N. Yusli, Z. Zolkapli

Centro de Investigacion y de Estudios Avanzados del IPN, Mexico City, Mexico

H. Castilla-Valdez, E. De La Cruz-Burelo, I. Heredia-De La Cruz³¹, R. Lopez-Fernandez, J. Mejia Guisao, A. Sanchez-Hernandez

Universidad Iberoamericana, Mexico City, Mexico

S. Carrillo Moreno, C. Oropeza Barrera, F. Vazquez Valencia

Benemerita Universidad Autonoma de Puebla, Puebla, Mexico

I. Pedraza, H. A. Salazar Ibarquen, C. Uribe Estrada

Universidad Autónoma de San Luis Potosí, San Luis Potosí, Mexico

A. Morelos Pineda

University of Auckland, Auckland, New Zealand

D. Krofcheck

University of Canterbury, Christchurch, New Zealand

P. H. Butler

National Centre for Physics, Quaid-I-Azam University, Islamabad, Pakistan

A. Ahmad, M. Ahmad, Q. Hassan, H. R. Hoorani, S. Qazi, A. Saddique, M. Shoaib, M. Waqas

National Centre for Nuclear Research, Swierk, Poland

H. Bialkowska, M. Bluj, B. Boimska, T. Frueboes, M. Górski, M. Kazana, K. Nawrocki, K. Romanowska-Rybinska, M. Szleper, P. Zalewski

Institute of Experimental Physics, Faculty of Physics, University of Warsaw, Warsaw, Poland

K. Bunkowski, A. Byszuk³², K. Doroba, A. Kalinowski, M. Konecki, J. Krolikowski, M. Misiura, M. Olszewski, A. Pyskir, M. Walczak

Laboratório de Instrumentação e Física Experimental de Partículas, Lisbon, Portugal

P. Bargassa, C. Beirão Da Cruz E Silva, B. Calpas, A. Di Francesco, P. Faccioli, M. Gallinaro, J. Hollar, N. Leonardo, L. Lloret Iglesias, M. V. Nemallapudi, J. Seixas, O. Toldaiev, D. Vadrucio, J. Varela

Joint Institute for Nuclear Research, Dubna, Russia

S. Afanasiev, P. Bunin, M. Gavrilenko, I. Golutvin, I. Gorbunov, A. Kamenev, V. Karjavin, A. Lanev, A. Malakhov, V. Matveev^{33,34}, V. Palichik, V. Perelygin, S. Shmatov, S. Shulha, N. Skatchkov, V. Smirnov, N. Voytishin, A. Zarubin

Petersburg Nuclear Physics Institute, Gatchina, St. Petersburg, Russia

Y. Ivanov, V. Kim³⁵, E. Kuznetsova³⁶, P. Levchenko, V. Murzin, V. Oreshkin, I. Smirnov, V. Sulimov, L. Uvarov, S. Vavilov, A. Vorobyev

Institute for Nuclear Research, Moscow, Russia

Yu. Andreev, A. Dermenev, S. Gninenko, N. Golubev, A. Karneyeu, M. Kirsanov, N. Krasnikov, A. Pashenkov, D. Tlisov, A. Toropin

Institute for Theoretical and Experimental Physics, Moscow, Russia

V. Epshteyn, V. Gavrilov, N. Lychkovskaya, V. Popov, I. Pozdnyakov, G. Safronov, A. Spiridonov, A. Stepenov, M. Toms, E. Vlasov, A. Zhokin

Moscow Institute of Physics and Technology, Moscow, Russia

T. Aushev, A. Bylinkin³⁴

National Research Nuclear University ‘Moscow Engineering Physics Institute’ (MEPhI), Moscow, Russia

M. Chadeeva³⁷, O. Markin, P. Parygin, D. Philippov, S. Polikarpov, V. Rusinov

P.N. Lebedev Physical Institute, Moscow, Russia

V. Andreev, M. Azarkin³⁴, I. Dremin³⁴, M. Kirakosyan³⁴, A. Terkulov

Skobeltsyn Institute of Nuclear Physics, Lomonosov Moscow State University, Moscow, Russia

A. Baskakov, A. Belyaev, E. Boos, M. Dubinin³⁸, L. Dudko, A. Ershov, A. Gribushin, V. Klyukhin, O. Kodolova, I. Lokhtin, I. Miagkov, S. Obraztsov, S. Petrushanko, V. Savrin, A. Snigirev

Novosibirsk State University (NSU), Novosibirsk, Russia

V. Blinov³⁹, Y. Skovpen³⁹, D. Shtol³⁹

State Research Center of Russian Federation, Institute for High Energy Physics, Protvino, Russia

I. Azhgirey, I. Bayshev, S. Bitioukov, D. Elumakhov, V. Kachanov, A. Kalinin, D. Konstantinov, V. Krychkin, V. Petrov, R. Ryutin, A. Sobol, S. Troshin, N. Tyurin, A. Uzunian, A. Volkov

Faculty of Physics and Vinca Institute of Nuclear Sciences, University of Belgrade, Belgrade, Serbia

P. Adzic⁴⁰, P. Cirkovic, D. Devetak, M. Dordevic, J. Milosevic, V. Rekovic

Centro de Investigaciones Energéticas Medioambientales y Tecnológicas (CIEMAT), Madrid, Spain

J. Alcaraz Maestre, M. Barrio Luna, M. Cerrada, N. Colino, B. De La Cruz, A. Delgado Peris, A. Escalante Del Valle, C. Fernandez Bedoya, J. P. Fernández Ramos, J. Flix, M. C. Fouz, P. Garcia-Abia, O. Gonzalez Lopez, S. Goy Lopez, J. M. Hernandez, M. I. Josa, A. Pérez-Calero Yzquierdo, J. Puerta Pelayo, A. Quintario Olmeda, I. Redondo, L. Romero, M. S. Soares, A. Álvarez Fernández

Universidad Autónoma de Madrid, Madrid, Spain

J. F. de Trocóniz, M. Missiroli, D. Moran

Universidad de Oviedo, Oviedo, Spain

J. Cuevas, C. Erice, J. Fernandez Menendez, I. Gonzalez Caballero, J. R. González Fernández, E. Palencia Cortezon, S. Sanchez Cruz, I. Suárez Andrés, P. Vischia, J. M. Vizán García

Instituto de Física de Cantabria (IFCA), CSIC-Universidad de Cantabria, Santander, Spain

I. J. Cabrillo, A. Calderon, B. Chazin Quero, E. Curras, M. Fernandez, J. Garcia-Ferrero, G. Gomez, A. Lopez Virto, J. Marco, C. Martinez Rivero, P. Martinez Ruiz del Arbol, F. Matorras, J. Piedra Gomez, T. Rodrigo, A. Ruiz-Jimeno, L. Scodellaro, N. Trevisani, I. Vila, R. Vilar Cortabitarte

CERN, European Organization for Nuclear Research, Geneva, Switzerland

D. Abbaneo, E. Auffray, P. Baillon, A. H. Ball, D. Barney, M. Bianco, P. Bloch, A. Bocci, C. Botta, T. Camporesi, R. Castello, M. Cepeda, G. Cerminara, E. Chapon, Y. Chen, D. d'Enterria, A. Dabrowski, V. Daponte, A. David, M. De Gruttola, A. De Roeck, E. Di Marco⁴¹, M. Dobson, B. Dorney, T. du Pree, M. Dünser, N. Dupont, A. Elliott-Peisert, P. Everaerts, G. Franzoni, J. Fulcher, W. Funk, D. Gigi, K. Gill, F. Glege, D. Gulhan, S. Gundacker, M. Guthoff, P. Harris, J. Hegeman, V. Innocente, P. Janot, O. Karacheban¹⁴, J. Kieseler, H. Kirschenmann, V. Knünz, A. Kornmayer¹¹, M. J. Kortelainen, C. Lange, P. Lecoq, C. Lourenço, M. T. Lucchini, L. Malgeri, M. Mannelli, A. Martelli, F. Meijers, J. A. Merlin, S. Mersi, E. Meschi, P. Milenovic⁴², F. Moortgat, M. Mulders, H. Neugebauer, S. Orfanelli, L. Orsini, L. Pape, E. Perez, M. Peruzzi, A. Petrilli, G. Petrucciani, A. Pfeiffer, M. Pierini, A. Racz, T. Reis, G. Rolandi⁴³, M. Rovere, H. Sakulin, C. Schäfer, C. Schwick, M. Seidel, M. Selvaggi, A. Sharma, P. Silva, P. Sphicas⁴⁴, J. Steggemann, M. Stoye, M. Tosi, D. Treille, A. Triossi, A. Tsiros, V. Veckalns⁴⁵, G. I. Veres¹⁶, M. Verweij, N. Wardle, W. D. Zeuner

Paul Scherrer Institut, Villigen, Switzerland

W. Bertl[†], K. Deiters, W. Erdmann, R. Horisberger, Q. Ingram, H. C. Kaestli, D. Kotlinski, U. Langenegger, T. Rohe, S. A. Wiederkehr

Institute for Particle Physics, ETH Zurich, Zurich, Switzerland

F. Bachmair, L. Bäni, P. Berger, L. Bianchini, B. Casal, G. Dissertori, M. Dittmar, M. Donegà, C. Grab, C. Heidegger, D. Hits, J. Hoss, G. Kasieczka, T. Klijsma, W. Lustermann, B. Mangano, M. Marionneau, M. T. Meinhard, D. Meister, F. Micheli, P. Musella, F. Nessi-Tedaldi, F. Pandolfi, J. Pata, F. Pauss, G. Perrin, L. Perrozzi, M. Quittnat, M. Rossini, M. Schönberger, L. Shchutska, A. Starodumov⁴⁶, V. R. Tavolaro, K. Theofilatos, M. L. Vesterbacka Olsson, R. Wallny, A. Zagozdinska³², D. H. Zhu

Universität Zürich, Zurich, Switzerland

T. K. Aarrestad, C. AMSLER⁴⁷, L. Caminada, M. F. Canelli, A. De Cosa, S. Donato, C. Galloni, T. Hreus, B. Kilminster, J. Ngadiuba, D. Pinna, G. Rauco, P. Robmann, D. Salerno, C. Seitz, A. Zucchetta

National Central University, Chung-Li, Taiwan

V. Candelise, T. H. Doan, Sh. Jain, R. Khurana, M. Konyushikhin, C. M. Kuo, W. Lin, A. Pozdnyakov, S. S. Yu

National Taiwan University (NTU), Taipei, Taiwan

Arun Kumar, P. Chang, Y. Chao, K. F. Chen, P. H. Chen, F. Fiori, W.-S. Hou, Y. Hsiung, Y. F. Liu, R.-S. Lu, M. Miñano Moya, E. Paganis, A. Psallidas, J. f. Tsai

Department of Physics, Faculty of Science, Chulalongkorn University, Bangkok, Thailand

B. Asavapibhop, K. Kovitanggoon, G. Singh, N. Srimanobhas

Cukurova University-Physics Department, Science and Art Faculty, Adana, Turkey

A. Adiguzel⁴⁸, F. Boran, S. Cerci⁴⁹, S. Damarseckin, Z. S. Demiroglu, C. Dozen, I. Dumanoglu, S. Girgis, G. Gokbulut, Y. Guler, I. Hos⁵⁰, E. E. Kangal⁵¹, O. Kara, A. Kayis Topaksu, U. Kiminsu, M. Oglakci, G. Onengut⁵², K. Ozdemir⁵³, D. Sunar Cerci⁴⁹, H. Topakli⁵⁴, S. Turkcapar, I. S. Zorbakir, C. Zorbilmez

Physics Department, Middle East Technical University, Ankara, Turkey

B. Bilin, G. Karapinar⁵⁵, K. Ocalan⁵⁶, M. Yalvac, M. Zeyrek

Bogazici University, Istanbul, Turkey

E. Gülmez, M. Kaya⁵⁷, O. Kaya⁵⁸, S. Tekten, E. A. Yetkin⁵⁹

Istanbul Technical University, Istanbul, Turkey

M. N. Agaras, S. Atay, A. Cakir, K. Cankocak

Institute for Scintillation Materials of National Academy of Science of Ukraine, Kharkov, Ukraine

B. Grynyov

National Scientific Center, Kharkov Institute of Physics and Technology, Kharkov, Ukraine

L. Levchuk, P. Sorokin

University of Bristol, Bristol, UK

R. Aggleton, F. Ball, L. Beck, J. J. Brooke, D. Burns, E. Clement, D. Cussans, H. Flacher, J. Goldstein, M. Grimes, G. P. Heath, H. F. Heath, J. Jacob, L. Kreczko, C. Lucas, D. M. Newbold⁶⁰, S. Paramesvaran, A. Poll, T. Sakuma, S. Seif El Nasr-storey, D. Smith, V. J. Smith

Rutherford Appleton Laboratory, Didcot, UK

K. W. Bell, A. Belyaev⁶¹, C. Brew, R. M. Brown, L. Calligaris, D. Cieri, D. J. A. Cockerill, J. A. Coughlan, K. Harder, S. Harper, E. Olaiya, D. Petyt, C. H. Shepherd-Themistocleous, A. Thea, I. R. Tomalin, T. Williams

Imperial College, London, UK

M. Baber, R. Bainbridge, S. Breeze, O. Buchmuller, A. Bundock, S. Casasso, M. Citron, D. Colling, L. Corpe, P. Dauncey, G. Davies, A. De Wit, M. Della Negra, R. Di Maria, P. Dunne, A. Elwood, D. Futyan, Y. Haddad, G. Hall, G. Iles, T. James, R. Lane, C. Laner, L. Lyons, A.-M. Magnan, S. Malik, L. Mastrolorenzo, T. Matsushita, J. Nash, A. Nikitenko⁴⁶, J. Pela, M. Pesaresi, D. M. Raymond, A. Richards, A. Rose, E. Scott, C. Seez, A. Shtipliyski, S. Summers, A. Tapper, K. Uchida, M. Vazquez Acosta⁶², T. Virdee¹¹, D. Winterbottom, J. Wright, S. C. Zenz

Brunel University, Uxbridge, UK

J. E. Cole, P. R. Hobson, A. Khan, P. Kyberd, I. D. Reid, P. Symonds, L. Teodorescu, M. Turner

Baylor University, Waco, USA

A. Borzou, K. Call, J. Dittmann, K. Hatakeyama, H. Liu, N. Pastika

Catholic University of America, Washington, DC, USA

R. Bartek, A. Dominguez

The University of Alabama, Tuscaloosa, USA

A. Buccilli, S. I. Cooper, C. Henderson, P. Rumerio, C. West

Boston University, Boston, USA

D. Arcaro, A. Avetisyan, T. Bose, D. Gastler, D. Rankin, C. Richardson, J. Rohlf, L. Sulak, D. Zou

Brown University, Providence, USA

G. Benelli, D. Cutts, A. Garabedian, J. Hakala, U. Heintz, J. M. Hogan, K. H. M. Kwok, E. Laird, G. Landsberg, Z. Mao, M. Narain, S. Piperov, S. Sagir, R. Syarif, D. Yu

University of California, Davis, CA, USA

R. Band, C. Brainerd, D. Burns, M. Calderon De La Barca Sanchez, M. Chertok, J. Conway, R. Conway, P. T. Cox, R. Erbacher, C. Flores, G. Funk, M. Gardner, W. Ko, R. Lander, C. Mclean, M. Mulhearn, D. Pellett, J. Pilot, S. Shalhout, M. Shi, J. Smith, M. Squires, D. Stolp, K. Tos, M. Tripathi, Z. Wang

University of California, Los Angeles, USA

M. Bachtis, C. Bravo, R. Cousins, A. Dasgupta, A. Florent, J. Hauser, M. Ignatenko, N. Mccoll, D. Saltzberg, C. Schnaible, V. Valuev

University of California, Riverside, CA, USA

E. Bouvier, K. Burt, R. Clare, J. Ellison, J. W. Gary, S. M. A. Ghiasi Shirazi, G. Hanson, J. Heilman, P. Jandir, E. Kennedy, F. Lacroix, O. R. Long, M. Olmedo Negrete, M. I. Paneva, A. Shrinivas, W. Si, L. Wang, H. Wei, S. Wimpenny, B. R. Yates

University of California, San Diego, La Jolla, USA

J. G. Branson, S. Cittolin, M. Derdzinski, B. Hashemi, A. Holzner, D. Klein, G. Kole, V. Krutelyov, J. Letts, I. Macneill, M. Masciovecchio, D. Olivito, S. Padhi, M. Pieri, M. Sani, V. Sharma, S. Simon, M. Tadel, A. Vartak, S. Wasserbaech⁶³, C. Welke, J. Wood, F. Würthwein, A. Yagil, G. Zevi Della Porta

University of California, Santa Barbara - Department of Physics, Santa Barbara, USA

N. Amin, R. Bhandari, J. Bradmiller-Feld, C. Campagnari, A. Dishaw, V. Dutta, M. Franco Sevilla, C. George, F. Golf, L. Gouskos, J. Gran, R. Heller, J. Incandela, S. D. Mullin, A. Ovcharova, H. Qu, J. Richman, D. Stuart, I. Suarez, J. Yoo

California Institute of Technology, Pasadena, USA

D. Anderson, J. Bendavid, A. Bornheim, J. M. Lawhorn, H. B. Newman, T. Nguyen, C. Pena, M. Spiropulu, J. R. Vlimant, S. Xie, Z. Zhang, R. Y. Zhu

Carnegie Mellon University, Pittsburgh, USA

M. B. Andrews, T. Ferguson, T. Mudholkar, M. Paulini, J. Russ, M. Sun, H. Vogel, I. Vorobiev, M. Weinberg

University of Colorado Boulder, Boulder, USA

J. P. Cumalat, W. T. Ford, F. Jensen, M. Krohn, S. Leontsinis, T. Mulholland, K. Stenson, S. R. Wagner

Cornell University, Ithaca, USA

J. Alexander, J. Chaves, J. Chu, S. Dittmer, K. McDermott, N. Mirman, J. R. Patterson, A. Rinkevicius, A. Ryd, L. Skinnari, L. Soffi, S. M. Tan, Z. Tao, J. Thom, J. Tucker, P. Wittich, M. Zientek

Fermi National Accelerator Laboratory, Batavia, USA

S. Abdullin, M. Albrow, G. Apollinari, A. Apresyan, A. Apyan, S. Banerjee, L. A. T. Bauerdick, A. Beretvas, J. Berryhill, P. C. Bhat, G. Bolla, K. Burkett, J. N. Butler, A. Canepa, G. B. Cerati, H. W. K. Cheung, F. Chlebana, M. Cremonesi, J. Duarte, V. D. Elvira, J. Freeman, Z. Gecse, E. Gottschalk, L. Gray, D. Green, S. Grünendahl, O. Gutsche, R. M. Harris, S. Hasegawa, J. Hirschauer, Z. Hu, B. Jayatilaka, S. Jindariani, M. Johnson, U. Joshi, B. Klima, B. Kreis, S. Lammel, D. Lincoln, R. Lipton, M. Liu, T. Liu, R. Lopes De Sá, J. Lykken, K. Maeshima, N. Magini, J. M. Marraffino, S. Maruyama, D. Mason, P. McBride, P. Merkel, S. Mrenna, S. Nahn, V. O'Dell, K. Pedro, O. Prokofyev, G. Rakness, L. Ristori, B. Schneider, E. Sexton-Kennedy, A. Soha, W. J. Spalding, L. Spiegel, S. Stoynev, J. Strait, N. Strobbe, L. Taylor, S. Tkaczyk, N. V. Tran, L. Uplegger, E. W. Vaandering, C. Vernieri, M. Verzocchi, R. Vidal, M. Wang, H. A. Weber, A. Whitbeck

University of Florida, Gainesville, USA

D. Acosta, P. Avery, P. Bortignon, A. Brinkerhoff, A. Carnes, M. Carver, D. Curry, S. Das, R. D. Field, I. K. Furic, J. Konigsberg, A. Korytov, K. Kotov, P. Ma, K. Matchev, H. Mei, G. Mitselmakher, D. Rank, D. Sperka, N. Terentyev, L. Thomas, J. Wang, S. Wang, J. Yelton

Florida International University, Miami, USA

Y. R. Joshi, S. Linn, P. Markowitz, G. Martinez, J. L. Rodriguez

Florida State University, Tallahassee, USA

A. Ackert, T. Adams, A. Askew, S. Hagopian, V. Hagopian, K. F. Johnson, T. Kolberg, T. Perry, H. Prosper, A. Santra, R. Yohay

Florida Institute of Technology, Melbourne, USA

M. M. Baarmand, V. Bhopatkar, S. Colafranceschi, M. Hohlmann, D. Noonan, T. Roy, F. Yumiceva

University of Illinois at Chicago (UIC), Chicago, USA

M. R. Adams, L. Apanasevich, D. Berry, R. R. Betts, R. Cavanaugh, X. Chen, O. Evdokimov, C. E. Gerber, D. A. Hangal, D. J. Hofman, K. Jung, J. Kamin, I. D. Sandoval Gonzalez, M. B. Tonjes, H. Trauger, N. Varelas, H. Wang, Z. Wu, M. Zakaria, J. Zhang

The University of Iowa, Iowa City, USA

B. Bilki⁶⁴, W. Clarida, K. Dilsiz⁶⁵, S. Durgut, R. P. Gandrajula, M. Haytmyradov, V. Khristenko, J.-P. Merlo, H. Mermerkaya⁶⁶, A. Mestvirishvili, A. Moeller, J. Nachtman, H. Ogul⁶⁷, Y. Onel, F. Ozok⁶⁸, A. Penzo, C. Snyder, E. Tiras, J. Wetzel, K. Yi

Johns Hopkins University, Baltimore, USA

B. Blumenfeld, A. Cocoros, N. Eminizer, D. Fehling, L. Feng, A. V. Gritsan, P. Maksimovic, J. Roskes, U. Sarica, M. Swartz, M. Xiao, C. You

The University of Kansas, Lawrence, USA

A. Al-bataineh, P. Baringer, A. Bean, S. Boren, J. Bowen, J. Castle, S. Khalil, A. Kropivnitskaya, D. Majumder, W. Mcbrayer, M. Murray, C. Royon, S. Sanders, E. Schmitz, R. Stringer, J. D. Tapia Takaki, Q. Wang

Kansas State University, Manhattan, USA

A. Ivanov, K. Kaadze, Y. Maravin, A. Mohammadi, L. K. Saini, N. Skhirtladze, S. Toda

Lawrence Livermore National Laboratory, Livermore, USA

F. Rebassoo, D. Wright

University of Maryland, College Park, USA

C. Anelli, A. Baden, O. Baron, A. Belloni, B. Calvert, S. C. Eno, C. Ferraioli, N. J. Hadley, S. Jabeen, G. Y. Jeng, R. G. Kellogg, J. Kunkle, A. C. Mignerey, F. Ricci-Tam, Y. H. Shin, A. Skuja, S. C. Tonwar

Massachusetts Institute of Technology, Cambridge, USA

D. Abercrombie, B. Allen, V. Azzolini, R. Barbieri, A. Baty, R. Bi, S. Brandt, W. Busza, I. A. Cali, M. D'Alfonso, Z. Demiragli, G. Gomez Ceballos, M. Goncharov, D. Hsu, Y. Iiyama, G. M. Innocenti, M. Klute, D. Kovalskyi, Y. S. Lai, Y.-J. Lee, A. Levin, P. D. Luckey, B. Maier, A. C. Marini, C. McGinn, C. Mironov, S. Narayanan, X. Niu, C. Paus, C. Roland, G. Roland, J. Salfeld-Nebgen, G. S. F. Stephans, K. Tatar, D. Velicanu, J. Wang, T. W. Wang, B. Wyslouch

University of Minnesota, Minneapolis, USA

A. C. Benvenuti, R. M. Chatterjee, A. Evans, P. Hansen, S. Kalafut, Y. Kubota, Z. Lesko, J. Mans, S. Nourbakhsh, N. Ruckstuhl, R. Rusack, J. Turkewitz

University of Mississippi, Oxford, USA

J. G. Acosta, S. Oliveros

University of Nebraska-Lincoln, Lincoln, USA

E. Avdeeva, K. Bloom, D. R. Claes, C. Fangmeier, R. Gonzalez Suarez, R. Kamalieddin, I. Kravchenko, J. Monroy, J. E. Siado, G. R. Snow, B. Stieger

State University of New York at Buffalo, Buffalo, USA

M. Alyari, J. Dolen, A. Godshalk, C. Harrington, I. Iashvili, D. Nguyen, A. Parker, S. Rappoccio, B. Roozbahani

Northeastern University, Boston, USA

G. Alverson, E. Barberis, A. Hortiangtham, A. Massironi, D. M. Morse, D. Nash, T. Orimoto, R. Teixeira De Lima, D. Trocino, R.-J. Wang, D. Wood

Northwestern University, Evanston, USA

S. Bhattacharya, O. Charaf, K. A. Hahn, N. Mucia, N. Odell, B. Pollack, M. H. Schmitt, K. Sung, M. Trovato, M. Velasco

University of Notre Dame, Notre Dame, USA

N. Dev, M. Hildreth, K. Hurtado Anampa, C. Jessop, D. J. Karmgard, N. Kellams, K. Lannon, N. Loukas, N. Marinelli, F. Meng, C. Mueller, Y. Musienko³³, M. Planer, A. Reinsvold, R. Ruchti, G. Smith, S. Taroni, M. Wayne, M. Wolf, A. Woodard

The Ohio State University, Columbus, USA

J. Alimena, L. Antonelli, B. Bylsma, L. S. Durkin, S. Flowers, B. Francis, A. Hart, C. Hill, W. Ji, B. Liu, W. Luo, D. Puigh, B. L. Winer, H. W. Wulsin

Princeton University, Princeton, USA

A. Benaglia, S. Cooperstein, P. Elmer, J. Hardenbrook, P. Hebda, S. Higginbotham, D. Lange, J. Luo, D. Marlow, K. Mei, I. Ojalvo, J. Olsen, C. Palmer, P. Piroué, D. Stickland, A. Svyatkovskiy, C. Tully

University of Puerto Rico, Mayagüez, USA

S. Malik, S. Norberg

Purdue University, West Lafayette, USA

A. Barker, V. E. Barnes, S. Folgueras, L. Gutay, M. K. Jha, M. Jones, A. W. Jung, A. Khatiwada, D. H. Miller, N. Neumeister, J. F. Schulte, J. Sun, F. Wang, W. Xie

Purdue University Northwest, Hammond, USA

T. Cheng, N. Parashar, J. Stupak

Rice University, Houston, USA

A. Adair, B. Akgun, Z. Chen, K. M. Ecklund, F. J. M. Geurts, M. Guilbaud, W. Li, B. Michlin, M. Northup, B. P. Padley, J. Roberts, J. Rorie, Z. Tu, J. Zabel

University of Rochester, Rochester, USA

A. Bodek, P. de Barbaro, R. Demina, Y. t. Duh, T. Ferbel, M. Galanti, A. Garcia-Bellido, J. Han, O. Hindrichs, A. Khukhunaishvili, K. H. Lo, P. Tan, M. Verzetti

The Rockefeller University, New York, USA

R. Ciesielski, K. Goulios, C. Mesropian

Rutgers, The State University of New Jersey, Piscataway, USA

A. Agapitos, J. P. Chou, Y. Gershtein, T. A. Gómez Espinosa, E. Halkiadakis, M. Heindl, E. Hughes, S. Kaplan, R. Kunnawalkam Elayavalli, S. Kyriacou, A. Lath, R. Montalvo, K. Nash, M. Osherson, H. Saka, S. Salur, S. Schnetzer, D. Sheffield, S. Somalwar, R. Stone, S. Thomas, P. Thomassen, M. Walker

University of Tennessee, Knoxville, USA

M. Foerster, J. Heideman, G. Riley, K. Rose, S. Spanier, K. Thapa

Texas A&M University, College Station, USA

O. Bouhali⁶⁹, A. Castaneda Hernandez⁶⁹, A. Celik, M. Dalchenko, M. De Mattia, A. Delgado, S. Dildick, R. Eusebi, J. Gilmore, T. Huang, T. Kamon⁷⁰, R. Mueller, Y. Pakhotin, R. Patel, A. Perloff, L. Perniè, D. Rathjens, A. Safonov, A. Tatarinov, K. A. Ulmer

Texas Tech University, Lubbock, USA

N. Akchurin, J. Damgov, F. De Guio, P. R. Dudero, J. Faulkner, E. Gurpinar, S. Kunori, K. Lamichhane, S. W. Lee, T. Libeiro, T. Peltola, S. Undleeb, I. Volobouev, Z. Wang

Vanderbilt University, Nashville, USA

S. Greene, A. Gurrola, R. Janjam, W. Johns, C. Maguire, A. Melo, H. Ni, P. Sheldon, S. Tuo, J. Velkovska, Q. Xu

University of Virginia, Charlottesville, USA

M. W. Arenton, P. Barria, B. Cox, R. Hirosky, A. Ledovskoy, H. Li, C. Neu, T. Sinthuprasith, X. Sun, Y. Wang, E. Wolfe, F. Xia

Wayne State University, Detroit, USA

C. Clarke, R. Harr, P. E. Karchin, J. Sturdy, S. Zaleski

University of Wisconsin - Madison, Madison, WI, USA

J. Buchanan, C. Caillol, S. Dasu, L. Dodd, S. Duric, B. Gomber, M. Grothe, M. Herndon, A. Hervé, U. Hussain, P. Klabbers, A. Lanaro, A. Levine, K. Long, R. Loveless, G. A. Pierro, G. Polese, T. Ruggles, A. Savin, N. Smith, W. H. Smith, D. Taylor, N. Woods

† Deceased

- 1: Also at Vienna University of Technology, Vienna, Austria
- 2: Also at State Key Laboratory of Nuclear Physics and Technology, Peking University, Beijing, China
- 3: Also at Universidade Estadual de Campinas, Campinas, Brazil
- 4: Also at Universidade Federal de Pelotas, Pelotas, Brazil
- 5: Also at Université Libre de Bruxelles, Brussels, Belgium
- 6: Also at Joint Institute for Nuclear Research, Dubna, Russia
- 7: Now at Cairo University, Cairo, Egypt
- 8: Also at Zewail City of Science and Technology, Zewail, Egypt
- 9: Also at Université de Haute Alsace, Mulhouse, France
- 10: Also at Skobeltsyn Institute of Nuclear Physics, Lomonosov Moscow State University, Moscow, Russia
- 11: Also at CERN, European Organization for Nuclear Research, Geneva, Switzerland
- 12: Also at RWTH Aachen University, III. Physikalisches Institut A, Aachen, Germany
- 13: Also at University of Hamburg, Hamburg, Germany
- 14: Also at Brandenburg University of Technology, Cottbus, Germany
- 15: Also at Institute of Nuclear Research ATOMKI, Debrecen, Hungary
- 16: Also at MTA-ELTE Lendület CMS Particle and Nuclear Physics Group, Eötvös Loránd University, Budapest, Hungary
- 17: Also at Institute of Physics, University of Debrecen, Debrecen, Hungary
- 18: Also at Indian Institute of Technology Bhubaneswar, Bhubaneswar, India
- 19: Also at Institute of Physics, Bhubaneswar, India
- 20: Also at University of Visva-Bharati, Santiniketan, India
- 21: Also at University of Ruhuna, Matara, Sri Lanka
- 22: Also at Isfahan University of Technology, Isfahan, Iran
- 23: Also at Yazd University, Yazd, Iran
- 24: Also at Plasma Physics Research Center, Science and Research Branch, Islamic Azad University, Tehran, Iran
- 25: Also at Università degli Studi di Siena, Siena, Italy
- 26: Also at INFN Sezione di Milano-Bicocca; Università di Milano-Bicocca, Milan, Italy
- 27: Also at Laboratori Nazionali di Legnaro dell'INFN, Legnaro, Italy
- 28: Also at Purdue University, West Lafayette, USA
- 29: Also at International Islamic University of Malaysia, Kuala Lumpur, Malaysia
- 30: Also at Malaysian Nuclear Agency, MOSTI, Kajang, Malaysia
- 31: Also at Consejo Nacional de Ciencia y Tecnología, Mexico City, Mexico
- 32: Also at Warsaw University of Technology, Institute of Electronic Systems, Warsaw, Poland
- 33: Also at Institute for Nuclear Research, Moscow, Russia
- 34: Now at National Research Nuclear University 'Moscow Engineering Physics Institute' (MEPhI), Moscow, Russia
- 35: Also at St. Petersburg State Polytechnical University, St. Petersburg, Russia

- 36: Also at University of Florida, Gainesville, USA
- 37: Also at P.N. Lebedev Physical Institute, Moscow, Russia
- 38: Also at California Institute of Technology, Pasadena, USA
- 39: Also at Budker Institute of Nuclear Physics, Novosibirsk, Russia
- 40: Also at Faculty of Physics, University of Belgrade, Belgrade, Serbia
- 41: Also at INFN Sezione di Roma; Sapienza Università di Roma, Rome, Italy
- 42: Also at University of Belgrade, Faculty of Physics and Vinca Institute of Nuclear Sciences, Belgrade, Serbia
- 43: Also at Scuola Normale e Sezione dell'INFN, Pisa, Italy
- 44: Also at National and Kapodistrian University of Athens, Athens, Greece
- 45: Also at Riga Technical University, Riga, Latvia
- 46: Also at Institute for Theoretical and Experimental Physics, Moscow, Russia
- 47: Also at Albert Einstein Center for Fundamental Physics, Bern, Switzerland
- 48: Also at Istanbul University, Faculty of Science, Istanbul, Turkey
- 49: Also at Adiyaman University, Adiyaman, Turkey
- 50: Also at Istanbul Aydin University, Istanbul, Turkey
- 51: Also at Mersin University, Mersin, Turkey
- 52: Also at Cag University, Mersin, Turkey
- 53: Also at Piri Reis University, Istanbul, Turkey
- 54: Also at Gaziosmanpasa University, Tokat, Turkey
- 55: Also at Izmir Institute of Technology, Izmir, Turkey
- 56: Also at Necmettin Erbakan University, Konya, Turkey
- 57: Also at Marmara University, Istanbul, Turkey
- 58: Also at Kafkas University, Kars, Turkey
- 59: Also at Istanbul Bilgi University, Istanbul, Turkey
- 60: Also at Rutherford Appleton Laboratory, Didcot, UK
- 61: Also at School of Physics and Astronomy, University of Southampton, Southampton, UK
- 62: Also at Instituto de Astrofísica de Canarias, La Laguna, Spain
- 63: Also at Utah Valley University, Orem, USA
- 64: Also at Beykent University, Istanbul, Turkey
- 65: Also at Bingol University, Bingol, Turkey
- 66: Also at Erzincan University, Erzincan, Turkey
- 67: Also at Sinop University, Sinop, Turkey
- 68: Also at Mimar Sinan University, Istanbul, Istanbul, Turkey
- 69: Also at Texas A&M University at Qatar, Doha, Qatar
- 70: Also at Kyungpook National University, Daegu, Korea